Please cite this article in press as: Song et al., Two-Dimensional Materials for Thermal Management Applications, Joule (2018), https://doi.org/10.1016/j.joule.2018.01.006

Joule

CellPress

Review

Two-Dimensional Materials for Thermal Management Applications

Houfu Song,[1,6] Jiaman Liu,[1,6] Bilu Liu,[1] Junqiao Wu,[1,2] Hui-Ming Cheng,[1,3,*] and Feiyu Kang[1,4,5,*]

With the advances of the electronics industry, the continuing trend of miniaturization and integration imposes challenges of efficient heat removal in nanoelectronic devices. Two-dimensional (2D) materials, especially graphene and hexagonal boron nitride (h-BN), are widely accepted as ideal candidates for thermal management materials due to their high intrinsic thermal conductivity and good mechanical flexibility. In this review, we introduce phonon dynamics of solid materials and thermal measurement methods at nanoscale, and highlight the unique thermal properties of 2D materials in relation to sample thickness, domain size, and interfaces. In addition, we discuss recent achievements of thermal management applications in which 2D materials act as heat spreader and thermal interface materials based on their controlled growth and self-assembly. Finally, critical consideration on the challenges and opportunities in thermal management applications of 2D materials is presented.

Introduction

Over the past century, modern electronics has undergone significant miniaturization and high-power densification, and the trend is still continuing.[1,2] Moore's law, which predicts that the number of transistors per square area will double in roughly every 18 months, continues to lead the pace of the semiconductor industry since it was put forward in the 1970s.[3] Significantly, this prediction on the development of electronics shows a direct relationship with heat dissipation. In industrial use, thermal design power (TDP) is defined as the maximum amount of heat that a chip can generate in its working condition, which serves as an important factor for chip design and thermal management in industry. It is easily recognized from some representative Intel microprocessors as a function of time (Figure 1) that the trend of increasing density of transistors and TDP is still continuing, leading to an unavoidable increase in temperature and significant reduction of device reliability.[4]

With rapid increase in power density in modern electronics, efficient heat removal has become an emerging demand for electronic devices including communication, information, and energy storage technologies because the higher a microprocessor's cooling rate, the faster it can operate and therefore operate with better performance. Ultra-fast high-frequency devices produce a large amount of heat in small localized areas, and thus generate hotspots where the working power can be over ten times higher than its average value.[5] As a result, deteriorated performance or even failure may occur on devices with low thermal conductivity, despite the relatively low operating temperatures of the majority of other regions.[6]

Thermal management is the effort to control the working temperature of devices such as integrated circuits (IC) by means of temperature monitoring and device cooling. As a broad definition, a thermal management setup is composed of a temperature controller, liquid/air cooling system, heat sink, and thermal interface materials

Context & Scale

Two-dimensional (2D) materials, especially graphene and hexagonal boron nitride (h-BN), have attracted great interest in thermal management as they exhibit superior thermal properties, in addition to other unique advantages of being atomically thin and mechanically flexible. Therefore, 2D materials are poised to potentially solve the increasingly severe heat dissipation problems in electronic and optoelectronic devices. Developing 2D material-based thermal interface materials with desired thermal properties has been extensively investigated. In this review, we focus on recent progress of integration of 2D materials into three-dimensional (3D) structures and their use as thermal interface materials as well as heat spreaders.

We first present the mechanism of thermal transport in 2D materials and advanced thermal characterization methods. The utilization of 2D materials with various composite forms for building phonon conduits is then reviewed. It is noteworthy that 3D structures constructed by purely 2D materials possess the highest thermal conductivity among all 3D composites. Finally, we summarize the challenges and opportunities, including interfacial engineering, 3D

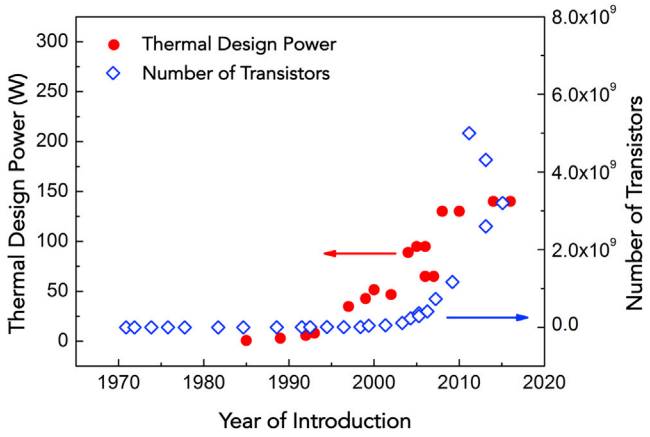

Figure 1. Timeline of Thermal Design Power and Number of Transistors for Intel Microprocessors
The data points show an overall exponential trend as a function of time consistent with Moore's law. Data were collected from Intel.[4]

(TIMs). Thermal management methodologies of hotspot removal include selection of materials with high thermal conductivity, as well as designing of heat sink and TIMs. The advance of these techniques is particularly related to the field of materials science, and is the topic of this review.

The rise of two-dimensional (2D) materials provides exciting opportunities for thermal management.[7,8] From inception in 2004, 2D materials such as graphene, hexagonal boron nitride (h-BN), transition metal dichalcogenides (TMDCs), and black phosphorous (BP) have attracted extensive interest from researchers and engineers because of their high surface area, good mechanical strength, and tunable physical properties.[9–12] As a result, 2D materials have shown great potential in a wide range of applications including thermal management, field-effect transistors, photodetectors, photovoltaic modules, energy storage devices, and catalysis.[13–19] In addition, these atomically thin materials show good mechanical properties and flatness due to their 2D nature, making them promising candidates for next-generation flexible electronic devices.[20,21] Impressively, it has been demonstrated that graphene shows ultrahigh thermal conductivity of 4,800–5,300 W m^{-1} K^{-1},[22,23] exceeding its bulk counterpart graphite, which already has a high thermal conductivity of ~2,000 W m^{-1} K^{-1}.[24] These results suggest the potential of graphene as a better choice for heat spreaders than commonly used metals.[25,26] Different from graphene, which has high thermal conductivity as well as electrical conductivity, h-BN is electrically insulating yet highly thermally conductive. These features make h-BN a superb candidate as a thermal management material for electronic devices on many practical occasions where electrical insulation is required.[27] From the physics point of view, 2D materials exhibit distinctive thermal properties from their bulk counterparts, such as ballistic[28,29] and hydrodynamic[30] transport of phonons at ~100 K. In addition, the intriguing phonon behavior provides an opportunity to update knowledge of heat transfer at the nanoscale. In summary, 2D materials with novel phonon properties, high thermal conductivity, and good mechanical flexibility are promising for both fundamental studies of heat transfer and thermal management applications in next-generation electronics.[31–33]

This review aims to provide an overview of fundamental phonon transport and thermal management applications of 2D materials. Basic phonon dynamics are presented first, followed by thermal measurement methods and thermal transport of 2D structure construction, and 2D device fabrication, for future research and development of thermal management in electronics.

[1]Shenzhen Environmental Science and New Energy Technology Engineering Laboratory, Shenzhen Geim Graphene Center (SGC), Tsinghua-Berkeley Shenzhen Institute (TBSI), Tsinghua University, Shenzhen 518055, China

[2]Department of Materials Science and Engineering, University of California, Berkeley, CA 94720, USA

[3]Shenyang National Laboratory for Materials Science, Institute of Metal Research, Chinese Academy of Sciences, Shenyang 110016, China

[4]Shenzhen Key Laboratory for Graphene-based Materials and Engineering Laboratory for Functionalized Carbon Materials, Shenzhen Geim Graphene Center (SGC), Graduate School at Shenzhen, Tsinghua University, Shenzhen 518055, China

[5]Laboratory of Advanced Materials, School of Materials Science and Engineering, Tsinghua University, Beijing 100084, China

[6]These authors contributed equally

*Correspondence: hmcheng@sz.tsinghua.edu.cn (H.-M.C.), fykang@sz.tsinghua.edu.cn (F.K.)

https://doi.org/10.1016/j.joule.2018.01.006

Please cite this article in press as: Song et al., Two-Dimensional Materials for Thermal Management Applications, Joule (2018), https://doi.org/10.1016/j.joule.2018.01.006

materials. We then introduce the use of 2D materials as thermal management materials, especially when used as TIMs and heat spreaders. In the last section, we discuss challenges and opportunities in thermal management from a material perspective. This review could serve as an introduction for interested readers to learn the thermal properties of 2D materials and their applications in thermal management.

Heat Transfer and Thermal Measurements in 2D Materials

Phonons and Thermal Transport in Solids at the Nanoscale

The capability of a material to conduct heat can be described by thermal conductivity κ through a macroscopic expression, i.e., Fourier 's law,

$$\vec{q} = -\kappa \nabla T , \qquad \text{(Equation 1)}$$

where q is the local heat flux and represents the amount of energy that flows through a unit area per unit time, and ∇T is the local temperature gradient.[34] It is widely accepted that in non-metals, heat is mainly carried by phonons, which are defined as the quanta of crystal lattice vibration.[35] Treating the vibrating lattice of a solid as a box of phonon gas, a simple kinetic model leads to the phonon-carried thermal conductivity,

$$\kappa = \frac{1}{3} C_v \upsilon l , \qquad \text{(Equation 2)}$$

where C_v is the specific heat of the lattice, υ is the phonon group velocity, and l is the mean free path of phonons in the material. Related to this equation is the concept of phonon dispersion, which shows the relationship between lattice vibration frequency ω and wavevector k, $\omega(k)$, and phonon group velocity υ is given by

$$\upsilon = \frac{\partial \omega_k}{\partial k} . \qquad \text{(Equation 3)}$$

The phonon dispersion relationship is vital for thermal transport studies as it bridges statistical atomic behavior to macroscopic heat flux. However, phonons can be scattered through anharmonicity of the lattice, including normal process (N) and Umklapp process (U) in crystal lattices,[36] and the latter one causes resistance to thermal transport. Notably, interfacial thermal property is particularly important for nanoscale thermal transport because nanoscale materials have high surface-to-volume ratios and are consequently more sensitive to interface than bulk materials. This makes interfacial thermal conductance, G_k, critical for thermal management in nanoscale materials. Thermal resistance at the interface is unavoidable even with atomically sharp and clean interfaces. Accordingly, the concept of Kapitza resistance is introduced as R_k, which measures thermal resistance caused by lattice mismatch across the interface.[37] Computational studies for solutions of Fourier 's law for 2D materials were first carried out based on the BTE.[35] It is especially useful for large system simulations, despite the fact that the phonon dispersion of a specific material is still needed and thus limits its applications. At the same time, molecular dynamics (MD) is introduced to study the atomistic picture of thermal transport.[38] As MD is compatible with anharmonic interaction simulations, it is widely used to investigate fundamental thermal properties of nanomaterials.

Methods of Thermal Conductivity Measurements

Thermal measurements at the nanoscale are extremely important yet challenging. The challenges include handling and controlling small specimens, poor accuracy of temperature and heat measurements at small scales, and the introduction of complicated devices that need precise control in their manufacturing process. It makes sense to make an analogy between thermal and electric measurements, except that electrically insulating material could be easily obtained and used as a

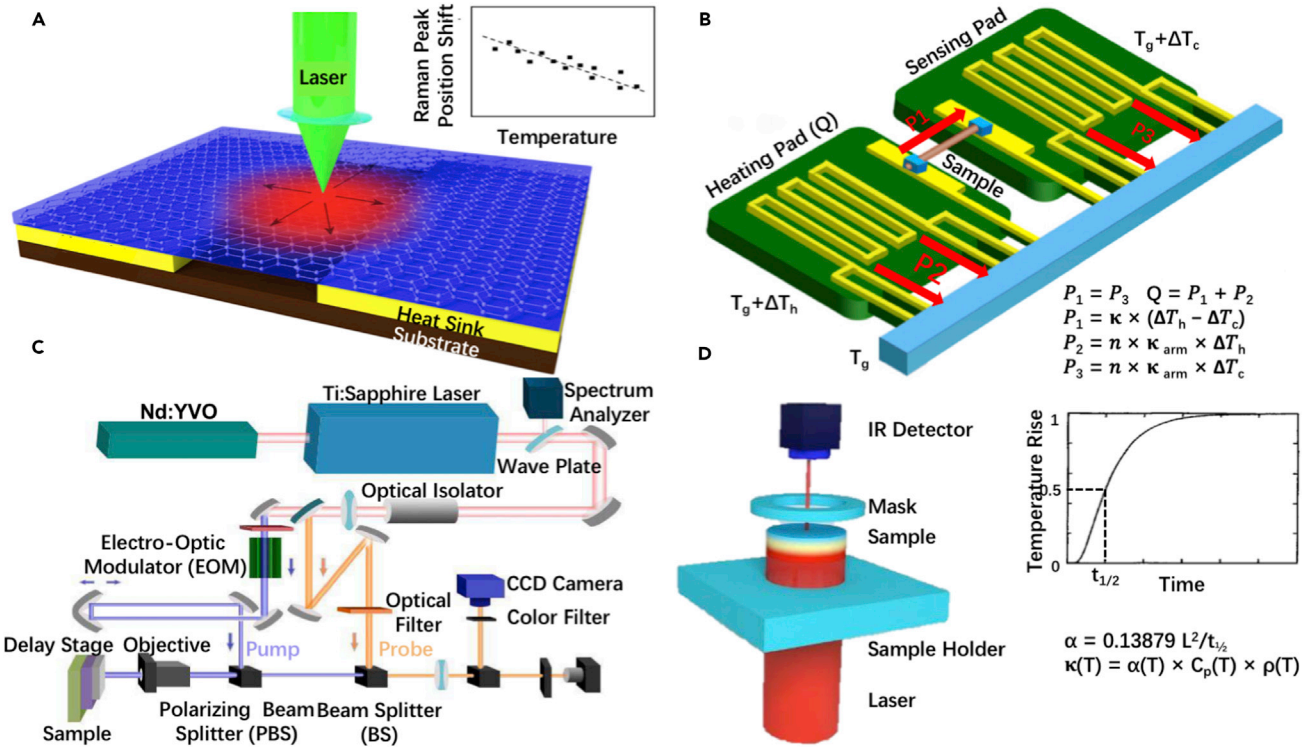

Figure 2. Scheme of Setups for Different Thermal Measurements

(A) Optothermal Raman method.

(B) Suspended-pad method.

(C) Time-domain thermoreflectance (TDTR) method, where blue and orange lines represent pump and probe laser beams, respectively.

(D) Laser flash method, where the left and right parts illustrate measurements of in-plane and cross-plane thermal conductivities.

Methods in (A) and (B) are steady-state methods, while those in (C) and (D) are transient methods.

substrate for electrical measurements, while no solid is sufficiently thermally insulating. As a result, distribution of heat flow between the sample and substrate must be carefully considered during the measurements. Instead of direct measurements of temperature, electrical[39,40] and optical[22,41] signals are usually measured and thermal properties are deduced from them. For more accurate measurements, heat radiation and convection in ambient air also need to be taken into consideration. To meet these challenges, various methods (Figure 2) have been developed for nanoscale thermal measurements in recent years. It should also be noted that detailed analysis of thermal measurement can be found in previous review papers.[7,8,42]

Optothermal Raman Method. The optothermal Raman technique was first used in 2008 by Balandin et al. to measure the in-plane thermal conductivity of a suspended single-layer graphene,[22] revealing a thermal conductivity as high as 4,800–5,300 W m^{-1} K^{-1}. In a typical measurement, a laser is used as a heat source and focused on the middle of a sample, causing a radial temperature gradient in the basal plane of 2D materials (Figure 2A). Because the peak shifts in Raman spectrum show linear relationship with the temperature change,[43] one can connect the temperature rise of the sample surface with the laser heating power, and the sample thermal conductivity can be calculated. It should be noted that the laser power absorbance of graphene with wavelength dependence is determined in different ways. In Balandin's work, a 488-nm laser was chosen for a clear Raman signal as

Please cite this article in press as: Song et al., Two-Dimensional Materials for Thermal Management Applications, Joule (2018), https://doi.org/10.1016/j.joule.2018.01.006

well as efficient heating effect, and the absorbed power for a specific laser was derived through an experimentally measured integrated Raman intensity in comparison with bulk graphite.[22] Some results were based on the difference between transmitted laser power through empty holes and graphene flakes,[44] or an assumption of 2.3% absorbance of laser power by graphene;[45] therefore, the observed results with data scattering are not surprising.

In addition to suspended graphene, thermal conductivity of substrate supported graphene was later measured by an optothermal Raman method.[19,25,44,45] As this method is optically based and non-destructive to the sample, it has been expanded to measure the thermal conductivity of other 2D materials including h-BN,[46] MoS_2,[47,48] and WS_2.[49] However, it should be noted that there are relatively high experimental errors in the optothermal Raman method. Such errors could result from inaccurate estimation of optical absorption of sample, uncertainty of laser spot size calibration, or the unavoidable heat dissipation to the surrounding environment and interfacial thermal conductance of supported area of samples. A modified method has been developed by carrying out measurements in a vacuum, which eliminates the influence of heat loss of surrounding gas.[50] Considering that the coefficient between Raman peak shift and temperature change is usually at the level of ~0.01 cm^{-1}/K for graphene, it is very challenging to determine both Raman shift and temperature change with high resolution.[43] In addition, detailed calculations are needed to further investigate physical processes behind the relationship of Raman peak shift and the sample temperature.

Suspended-Pad Method. A micropad method was developed to measure thermal conductivity of carbon nanotubes (CNTs) as early as 2001.[39] The device (Figure 2B) is made of two silicon nitride (SiN_x) membranes, with a platinum (Pt) serpentine line patterned on each pad and used as microheaters and thermometers, providing Joule heating and calibrating temperature of the two pads, respectively. The pads are suspended by six SiN_x arms coated with Pt for electrical and thermal conductivity measurements. The sample, which is usually a nanoribbon or nanowire, is then transferred by a sharp tip under a microscope to bridge the two micropads. The sample is then bonded onto a Pt electrode by focused ion beam to ensure Ohmic contacts and minimize thermal resistance. Heat transfer in the sample can be calculated from Joule heating of the heated pad and temperature rise of the other, sensing pad.

This suspended-pad method has also been used to measure the thermal conductivity of 2D materials including graphene, h-BN, MoS_2, BP, and Bi_2Te_3.[51–56] This method shows straightforward and reliable calibration on temperature with high resolution (~0.05 K),[57] which makes it a powerful technique for in-plane thermal conductivity measurements. However, the accuracy of this technique can be significantly affected by polymer residues on 2D materials,[58,59] and the tip-assisted sample transfer would be technically challenging and time consuming. The device fabrication process is also complicated.[55]

Time-Domain Thermoreflectance Method. The time-domain thermoreflectance (TDTR) method is a "pump-probe" optical technique to measure thermal transport at nanoscale thickness. Although the first report can be dated back to 1986,[41] it was extensively studied only in recent years with the rise of nanomaterials.[60,61] In a typical measurement, a mode-locked laser is split into a "pump" beam and a "probe" beam. The pump beam produces a temperature rise of ~3 K near the metallic surface (either the sample is metallic or is coated with a thin metal film). The probe beam, which is in the middle of pump, can monitor surface temperature

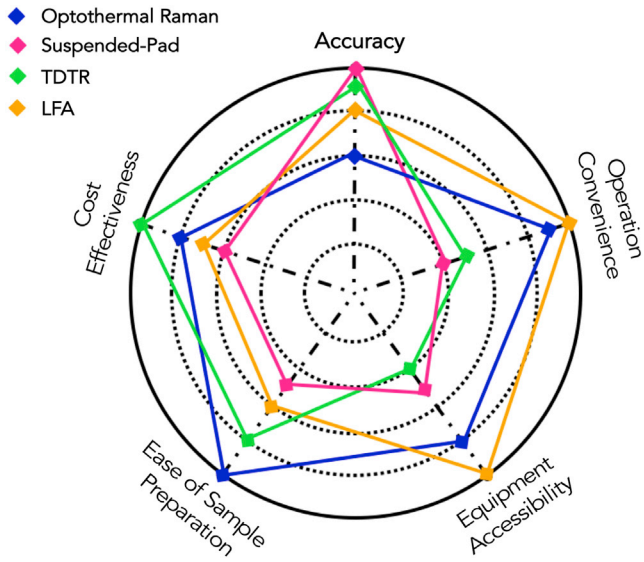

Figure 3. Comparison of Four Commonly Used Methods for Thermal Conductivity Measurements, Graded in Terms of Their Relative Accuracy, Operation Convenience, Equipment Accessibility, Ease of Sample Preparation, and Cost Effectiveness

with the change of optical reflectivity. The phase and amplitude of the probe are measured as a function of delay time between the pump and probe, and output by a lock-in amplifier (Figure 2C). A mathematical fitting is then conducted to extract thermal parameters. The resolution of heat penetration at the nanoscale makes TDTR a powerful method for interface thermal transport measurement,[62] among which the most intensively studied sample is graphene/metal interface.[63–68] TDTR has also been reported to be able to measure cross-plane thermal conductivity of 2D materials such as BP[69] and WSe_2.[70]

Other Methods. Besides the methods discussed above, there are some other commercial instruments based on micrometer-scale resolution that could be modified for thermal measurements at the nanoscale. For example, a scanning thermal microscope (SThM) is a specially designed scanning probe microscope that gives a temperature mapping result based on a sharp scanning tip. It was first used for thermal conductivity measurement of CNTs in 2000.[71] Null point scanning thermal microscopy (Np SThM) was modified by measuring the local heat transported from the sample to the tip only, minimizing the impact of heat transfer in the air gap between the sample and tip.[72] With this method, a residue-free suspended graphene was measured and showed a thermal conductivity of ~2,400 $W\,m^{-1}\,K^{-1}$ at room temperature.[73] For bulk materials, one of the most widely used commercial devices is the laser flash apparatus. In this setup, the sample is cut to a specific size and heated by a pulse laser, and the thermal diffusivity can then be measured by manipulation of the thickness of the sample and thermal diffusion time (Figure 2D). It is a convenient way for thermal measurements provided that the sample size meets the requirements,[28,74] and is especially useful for characterization of thermal management materials for real application. The advantages and disadvantages of different thermal conductivity measurement methods are summarized in Figure 3.

Thermal Transport in 2D Materials

Phonon Dispersion. In 2D materials, because most of them are semiconductors, heat is mainly transported by phonons due to the absence of high density of free

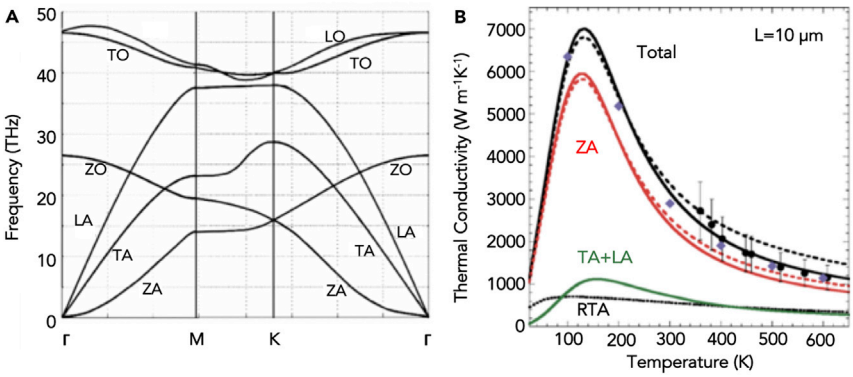

Figure 4. Theoretical Investigation of Phonons in Graphene

(A) Phonon dispersion of graphene by the valence-force field method. TA, transverse acoustic phonons; LA, longitudinal acoustic phonons; ZA, out-of-plane acoustic phonon branch; LO, longitudinal optical phonons; TO, transverse optical phonons; ZO, out-of-plane optical phonons. Reprinted from Nika et al.,[35] with permission. Copyright 2009, American Physical Society.

(B) Calculated thermal conductivity and the contributions of different phonon modes for graphene with a channel length of L = 10 μm. The solid black curve[85] and dashed black curve[83] give theoretical results while black circles are experimental data for single-layer suspended graphene.[50] The lower dotted black curve gives thermal conductivity by relaxation time approximation (RTA). Reprinted from Lindsay et al.,[85] with permission, Copyright 2014, American Physical Society.

electrons. Even in graphene, which is a semi-metal, phonons rather than electrons are the main heat carriers. Due to the strong covalent sp^2 bonding between carbon atoms, heat conduction is very efficient in its basal plane.[75] The much weaker van der Waals forces between the atomic layers compared with the covalent bonding in the basal plane leads to very anisotropic thermal conductivity for 2D materials between the x-y plane (in-plane) and along the z direction (cross-plane).[76] It was also theoretically predicted that some 2D materials could show anisotropic thermal properties in the basal x-y plane,[77,78] which was later experimentally observed in BP.[55,79] Klemens has calculated the intrinsic in-plane thermal conductivity of graphite[75,80] and found it to be ~1,910 W m^{-1} K^{-1} at room temperature, which is close to the previous experimental result of highly oriented pyrolytic graphite of 1,850 W m^{-1} K^{-1}.[81] In this model, out-of-plane acoustic phonon branch (ZA) of graphite was neglected due to its low phonon velocity and high Gruneisen factor γ,[82] while assuming that heat is dominantly carried by transverse acoustic phonons and longitudinal acoustic phonons (Figure 4A). However, this assumption was challenged by later studies, arguing that the ZA phonons are dominant in thermal conduction in 2D materials including graphene and h-BN.[83,84] This behavior is attributed to a selection rule that restricts the phonon scattering of ZA phonons,[83] and shows consistency with experimentally measured results of SiO_2 supported graphene (Figure 4B).[50,52,85] Overall, this has been updated by recent papers reporting that ZA phonons dominate in heat transfer in 2D materials in the in-plane direction. However, experimental investigation of the roles of different phonons in thermal conduction is still needed for a full understanding of thermal conduction physics of 2D materials.

Effect of Thickness. Thickness-dependent thermal conductivity of suspended graphene was first reported by Ghosh et al.[86] using the optothermal Raman method, and the results show a drop from ~2,800 to ~1,300 W m^{-1} K^{-1} as the number of graphene layers increases from 2 to 4. However, when graphene is supported by amorphous SiO_2, it shows rising thermal conductivity in parallel with increasing thickness.[87] The difference is attributed to distinct limitations of phonon transport in each case. In the suspended case, thermal transport is limited by intrinsic

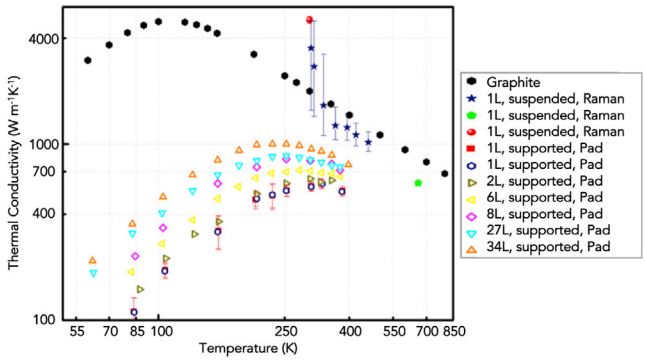

Figure 5. Experimental Results of In-Plane Thermal Conductivity of Graphene as a Function of Temperature and Different Number of Layers

The optothermal Raman technique by Balandin et al.,[22] Lee et al.,[88] and Faugeras et al.,[45] and the suspended-pad method by Seol et al.[52] and Sadeghi et al.[87] are included. Bulk graphite by Touloukian[24] is shown for comparison. Only results from mechanically exfoliated graphene are presented here, because other methods may produce graphene with lower quality than that of mechanically exfoliated ones.

properties, and an increased Umklapp scattering was discovered in thicker-layer graphene due to crystal anharmonicity; in contrast, in the supported case the extrinsic property is dominant, as the phonon-interface scattering leads to a suppression of phonon modes, especially the ZA modes, which would contribute most to the thermal transport.[83,88] The above measurements are summarized in Figure 5, and more details of phonon behaviors deciding thickness-dependent thermal conductivity of graphene can be found elsewhere.[7] Meanwhile, the reduction of thermal conductivity at small thicknesses has been found in suspended h-BN[51] and MoS_2,[54] and was explained by increasing phonon scattering with polymer residues on the surface.[51] Further investigation of thickness-related thermal conductivity measurements is needed to elucidate these effects, as it could provide fundamental knowledge on thermal properties of 2D materials and their applications in thermal management.

Effect of Domain Size. Intensive experimental and theoretical efforts have also been directed toward the effect of domain size on thermal properties. In the Klemens model, in-plane thermal conductivity of graphite shows a logarithmic divergence with the grain size.[75] Based on an ideal case where heat transfer is only inhibited by Umklapp scattering, simulation study indicates that the thermal conductivity of graphene can exceed the bulk limit provided that the flake domain size is up to a few micrometers.[89] This trend has been confirmed by a suspended-pad measurement, showing that the thermal conductivity keeps logarithmically increasing even if the sample length reaches 10 μm, much longer than the mean free path.[53] For larger domain sizes (~30 μm), a finite value was discovered by theoretical study.[90] In real cases, phonons would be scattered by defects besides the Umklapp scattering.[91] Nevertheless, the theoretical studies point to ways of improving the thermal conductivity by growing large crystals of 2D materials.[92]

Heterostructures and Interfaces. Van der Waals heterostructures assembled with 2D materials has attracted great attention because of their interesting science and potential applications in electronics, optoelectronics, and thermal managements.[93] Both vertical and lateral 2D heterostructures have been synthesized, with an atomically flat surface three times smoother than SiO_2 (Figure 6A), and a sharp edge that is observed in high-angle annular dark field (HAADF) transmission electron

Please cite this article in press as: Song et al., Two-Dimensional Materials for Thermal Management Applications, Joule (2018), https://doi.org/10.1016/j.joule.2018.01.006

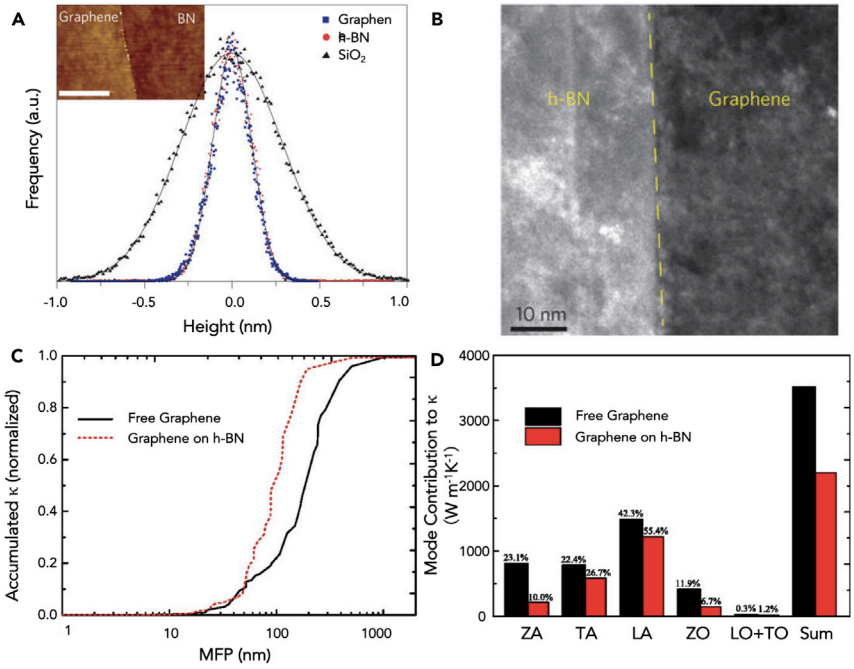

Figure 6. Characterization and Calculated Thermal Transport Property of Graphene/h-BN Heterostructures

(A) Histogram of the surface roughness of SiO_2 (black triangles), h-BN (red circles), and graphene-on-BN vertical heterostructures (blue squares) measured by atomic force microscopy (AFM). Solid lines are Gaussian fits to the distribution of height. Inset: a high-resolution AFM image showing graphene on an h-BN substrate. Reprinted from Dean et al.,[96] with permission. Copyright 2010, Nature Publishing Group.

(B) A HAADF TEM image of a graphene/h-BN lateral heterostructure. The left part is h-BN and the right part is graphene. Comparison of thermal conductivity of free and h-BN-supported graphene is shown. Reprinted from Liu et al.,[94] with permission. Copyright 2013, Nature Publishing Group.

(C) Thermal conductivity as a function of mean free path (MFP) of graphene and h-BN. Reprinted from Zou and Cao.,[98] with permission. Copyright 2017, AIP Publishing LLC.

(D) Phonon mode contribution to thermal conductivity of free graphene (black) and graphene on h-BN (red). Reprinted from Zou and Cao.,[98] with permission. Copyright 2017, AIP Publishing LLC.

microscopy (TEM) image as shown in Figure 6B.[94,95] Among these, graphene/BN vertical heterostructures have been extensively studied since they show the highest charge carrier mobility of graphene supported on any substrate.[96] Meanwhile, phonon and thermal studies of heterostructures are of great interest for nanoelectronic applications.[97]

Interface thermal conductance of graphene/h-BN interface was measured to be ~52 MW m^{-2} K^{-1} by the optothermal Raman method, higher than that of MoS_2/h-BN interface (17 MW m^{-2} K^{-1}) due possibly to strong cross-plane transmission of phonon modes at the interface.[99] However, it was measured that the interface thermal conductance of graphene/SiO_2 interface is roughly equal to or higher than that of graphene/h-BN.[100,101] Although the inconsistency is dominantly attributed to experimental uncertainties for different measurement methods and variation in sample quality difference, it is still intriguing to explore intrinsic thermal transport properties from the perspective of lattice configurations at the interface.[102] It is suggested that intercoupling between graphene and h-BN is not strong, thus leading to failure of the symmetry-based selection rule, significantly reducing the lifetime of ZA phonons of supported graphene (Figures 6C and 6D).[98] Interfacial reinforcement

Please cite this article in press as: Song et al., Two-Dimensional Materials for Thermal Management Applications, Joule (2018), https://doi.org/10.1016/j.joule.2018.01.006

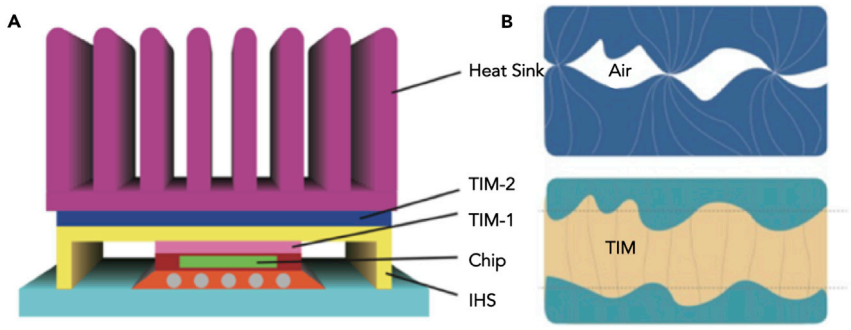

Figure 7. Schematic of an IC and Role of TIMs

(A) Illustration of a typical IC package with two TIMs and one integrated heat spreader (IHS). The TIMs are applied between chip/IHS and IHS/heat sink interfaces and defined as TIM-1 and TIM-2, respectively.

(B) Schematic of a TIM. An interface in the absence of TIM (top) shows conjunct heat flux, with heat transfer at limited solid contact areas.

can be achieved by stacking for more C-B matching to reduce interfacial space,[103] or specifically introducing 5|7 carbon defects to relax the lattice mismatch.[104] However, most work on this topic is based on computational methods and corresponding experimental investigations are urgently required.

Other Factors. In addition to the above factors that have significant influence on the thermal conductivity of 2D materials, other factors, including isotopic modification,[105] ion intercalating,[106] tensile strain,[107] defect engineering,[108] and functionalization,[109] can also be used to engineer the thermal conductivity of 2D materials. These are shown to exist mainly on graphene, but in principle they should work for other 2D materials as well.

2D Materials for Thermal Management

2D Materials as Fillers for Polymer-Based TIMs. A typical thermal management system in IC chips is depicted in Figure 7A. It contains a heat sink, an integrated heat spreader (IHS), and two TIMs named as TIM 1 and TIM 2. A TIM is used to connect two solid materials together by filling in the air gap between them, and thus reduces the interfacial thermal resistance (Figure 7B). In accordance with the package structure, TIMs can be categorized into several groups including polymer-based composites, solders, and other materials.[110] Among them, polymer-based composites with epoxy, silicone, poly(methyl methacrylate) (PMMA) and poly(vinyl alcohol) (PVA) matrix are most widely used due to their good adaptability to versatile solid interfaces. While polymers themselves generally have low thermal conductivities (<0.5 W m^{-1} K^{-1}), fillers with relatively high thermal conductance capabilities such as ceramics,[111–113] carbon materials,[114,115] and metals[116] are incorporated, exhibiting overall thermal conductivities in the range of 1–10 W m^{-1} K^{-1}.[117] 2D materials such as graphene[118–120] and h-BN[27,121–123] were reported to be promising candidates for highly thermal conductive fillers of polymer-based TIMs. These TIMs could also be applied on energy devices including batteries and solar cells.[124–126]

Achieving uniform dispersion of 2D materials in a polymer matrix is of great significance in fabricating high-performance polymer-based TIMs. Typically, a TIM with high thermal conductivity requires high filler loading (up to 90 wt%) to exceed the percolation threshold, i.e., forming a thermal conductive path inside the polymer matrix.[127] High loading is also beneficial as it increases the surface area of highly thermal conductive fillers, since the practical indicator of heat removal ability, the

Please cite this article in press as: Song et al., Two-Dimensional Materials for Thermal Management Applications, Joule (2018), https://doi.org/10.1016/j.joule.2018.01.006

thermal conductance, scales linearly with both thermal conductivity and cross-section area. However, overloading of fillers could result in a loss of mechanical properties of composites; therefore, minimizing filler loading while keeping high thermal conductivity is always a preference for practical use, but remains a technical challenge. To achieve this, one has to make fillers well dispersed in the polymer matrix so that the interface thermal resistance between filler and matrix would be reduced, while the process is highly related to the preparation methods of materials. 2D material fillers are generally prepared by a liquid exfoliation process, including chemically modified exfoliation for graphene oxide (GO)[128,129] and functionalized h-BN nanosheets,[130,131] and direct sonication of pristine bulk materials in solvents.[132–136] Exfoliation of chemically modified layered materials often yields good dispersion of 2D materials with high concentration, but inevitably introduces defects in the materials. On the other hand, direct exfoliation of pristine bulk materials can produce 2D materials with high quality, although the prepared samples are difficult to disperse in the polymer matrix at high concentrations because of their high cohesive energy of van der Waals force.[137,138] Therefore, there is a trade-off between preparing high-quality fillers and building a good filler-matrix interface. In the following, methods of reaching high intrinsic thermal conductivity and enhancing the thermal interface are discussed separately.

Improvement in dispersity is very important to achieve uniform and stable dispersion of 2D fillers into a polymer matrix and consequently improve the thermal conductivity of the system. Chemical modification of 2D materials functionalizes the 2D nanosheets and therefore improves their dispersity in polymer matrices. Covalent bonding can be introduced by grafting functional groups or molecules including amines,[139] silane,[140] and polymer monomers[141] onto 2D materials. However, this method is used at the expense of reducing the intrinsic thermal conductivity of 2D materials.[142] Non-covalent functionalization by solvent-soluble molecules is an alternative method. For example, benzene derivatives are usually used to introduce π-π stacking with graphene while the other side of the molecule is compatible with the polymer matrix,[120,143] leading to a system with improved interface thermal transport while not degrading the intrinsic thermal conductivity of graphene itself. Methods to modify graphene and GO have been well developed and reviewed in recent publications.[144,145] At the same time, mechanical techniques can be introduced for improved dispersion and high loading of 2D materials in polymer matrices. An external force can be applied by means of tip sonication,[146] vacuum filtration mixing,[147,148] hot-pressing,[149] and so forth.

Building phonon conduits is another important aspect for enhancement of the filler-polymer interface, which can be realized by the formation of hybrid structures of low-dimensional materials including graphene, h-BN, and CNTs. It was discussed in a previous section that graphenes with larger domain sizes show higher thermal conductivity than those with smaller ones. 2D materials with large domain sizes are therefore desirable, because they form a filler structure that reaches the thermal percolation threshold with less interface area.[150] However, solely applying fillers with large sizes may fail to form a complete heat pathway in the whole polymer matrix because of limited overlapping areas between the nanosheets of 2D materials. Therefore, the concept of building hybrid structures has been suggested, with microsize and nanosize fillers functioning as brick and cement for phonon conduits, respectively. Hybrid fillers with graphene and CNTs have attracted extensive attention since its first report in 2008.[118] A high loading of graphene and CNTs with synergic effect was later reported with a loading of 20 vol% each, showing a thermal conductivity of 6.18 W m^{-1} K^{-1}, which is higher than that of 50 vol% individual

Please cite this article in press as: Song et al., Two-Dimensional Materials for Thermal Management Applications, Joule (2018), https://doi.org/10.1016/j.joule.2018.01.006

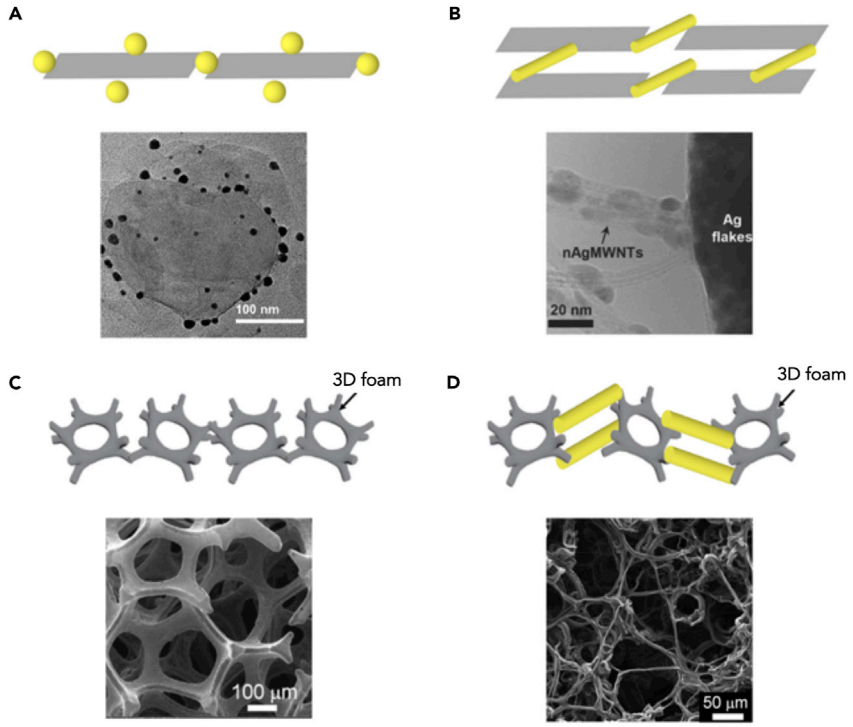

Figure 8. 2D Materials in Polymer-Based TIMs with Hybrid and Interconnected Structures

(A–D) Schematic and experimental results are shown at top and bottom of each column separately.

(A) 2D nanosheets combined with nanoparticles. Reprinted from Wang et al.,[152] with permission. Copyright 2016, Nature Publishing Group.

(B) 2D nanosheets combined with 1D nanotubes. Reprinted from Suh et al.,[153] with permission. Copyright 2016, Wiley.

(C) 3D foam structure. Reprinted from Kholmanov et al.,[155] with permission. Copyright 2015, American Chemical Society.

(D) 3D foam structure with 1D nanotube connection. Reprinted from Kholmanov et al.,[155] with permission. Copyright 2015, American Chemical Society.

CNTs or graphene.[146] Building a micro-nano-size hybrid structure with different shapes of fillers shows improved thermal conductivity, and these examples include graphene flakes with Ag particles,[151,152] h-BN flakes with SiC nanowires,[148] and Ag flakes with CNTs[153] (Figures 8A and 8B). Simulations show that a microsize filler is substantial for reaching percolation threshold due to its large contact surface areas with polymer matrix,[154] which is consistent with experimental results mentioned above.

Another effective method to build phonon conduits is to form 3D interconnected structures. In recent years, construction of thermally conductive 3D interconnected networks has become a new research frontier in TIM design. Compared with methods mentioned above, filling a highly thermally conductive 3D structure requires lower filler loading to reach percolation threshold. Several methods have been reported to synthesize 3D macroforms of graphene and h-BN, such as direct growth by chemical vapor deposition (CVD) using Ni foam as a template,[156] and self-assembly of GO.[157,158] CVD produces graphene foams (GFs) with a highly crystalline structure. A GF/wax composite shows improved thermal conductivity of 2.13 W m^{-1} K^{-1}, which is up to 18-fold enhancement compared with bare wax, at an ultralow GF loading of 1.23 vol%.[159] This value can be further increased by 1.8-fold when the porous space of GFs is occupied by long CNTs, forming

Please cite this article in press as: Song et al., Two-Dimensional Materials for Thermal Management Applications, Joule (2018), https://doi.org/10.1016/j.joule.2018.01.006

Table 1. Comparisons of Thermal Conductivities of Polymer-Based TIMs with Different Fillers

Fillers	Loading	K (W m^{-1} K^{-1})	Method	Reference
Filler Modification				
rGO	25 vol%	6.44	–	Yu et al.[115]
rGO	20 wt%	5.8	silane functionalized	Ganguli et al.[140]
Graphene	10 vol%	5.1	sodium cholate functionalized	Shahil et al.[119]
Graphene	10 wt%	1.53	pyrene derivatives functionalized	Song et al.[143]
rGO	4 wt%	1.91	pyrene derivatives functionalized	Teng et al.[120]
h-BN nanotube	30 wt%	2.77	CVD grown, silane functionalized	Huang et al.[123]
Forced Mixing				
h-BN	94 wt%	6.9 ($\kappa_{\perp}$)	[PVA] vacuum filtrated	Zeng et al.[147]
GO	10 wt%	0.244 ($\kappa_{\perp}$)	hot pressed	Ding et al.[149]
Hybrid Filler				
Graphene + CNT	7.5 wt% + 2.5 wt%	1.75	GNP, single-walled carbon nanotube	Yu et al.[118]
Graphene + CNT	20 vol% + 20 vol%	6.31	GNP, multiwalled carbon nanotube	Huang et al.[146]
Ag flake + CNT	35.8 vol% +2.3 vol%	160	Ag-nanoparticle-functionalized CNT	Suh et al.[153]
h-BN + SiC nanowire	95 wt%	21.7	[PVA] vacuum filtrated	Yao et al.[148]
3D Interconnected Structure				
Graphene	1.23 vol%	3.44	[wax] CVD grown, annealed	Ji et al.[159]
Graphene + CNT	15.8 vol% (in total)	4.09	[erythritol] CVD grown, annealed	Kholmanov et al.[155]
h-BN	1.5 vol%	1.03	[PMMA] CVD grown	Xue et al.[160]
rGO	0.92	2.13	aligned freeze drying, 400°C reduced	Lian et al.[163]
h-BN	9.29	2.8	aligned freeze drying	Zeng et al.[162]

Epoxy resin was used as matrix unless otherwise specified.

concentrated heat transfer channels in GF/CNT/polymer composites (Figures 8C and 8D).[155] Similarly, 3D h-BN foam has been grown by Ni foam-templated CVD,[160] and showed nearly 3-fold improvement of thermal conductivity in h-BN/PMMA composites.[161] Based on GO dispersion, the solution method is an alternative way to produce 3D connected filler networks. Using an ice-templated method, an alternative way to produce 3D connected filler networks was accomplished by promptly contacting the hydrogel with cold medium, creating a 3D network with preferred structure orientation.[162,163] Typical thermal conductivities of polymer-based TIM with 2D materials fillers are summarized in Table 1. Solution-induced aerogel is easy to be scaled up at relatively low cost, despite the fact that the functionalization of graphene and BN nanosheets degrades their high intrinsic thermal conductivity. The aerogel needs to be annealed properly in order to recover the thermal conductivity of pristine graphene/h-BN as much as possible, while retaining the mechanical strength of as-prepared monolith. Efforts have been devoted to improving the loading fraction by condensing the aerogel,[164] or controllable synthesis for anisotropic thermal conductive frameworks.[165] Many other factors are also essential for real applications such as clamping pressure, cycle ability, and liquid leakage. These indicators are primarily related to industrial technology and are therefore beyond the scope of this paper. However, it is worth noting when designing real thermal management applications.

Direct Use of 2D Materials and Their 3D Assembly for Thermal Management

Graphene and h-BN filled TIMs have shown significantly enhanced thermal conductivity compared with commercial ones. However, the overall performance is still far

Please cite this article in press as: Song et al., Two-Dimensional Materials for Thermal Management Applications, Joule (2018), https://doi.org/10.1016/j.joule.2018.01.006

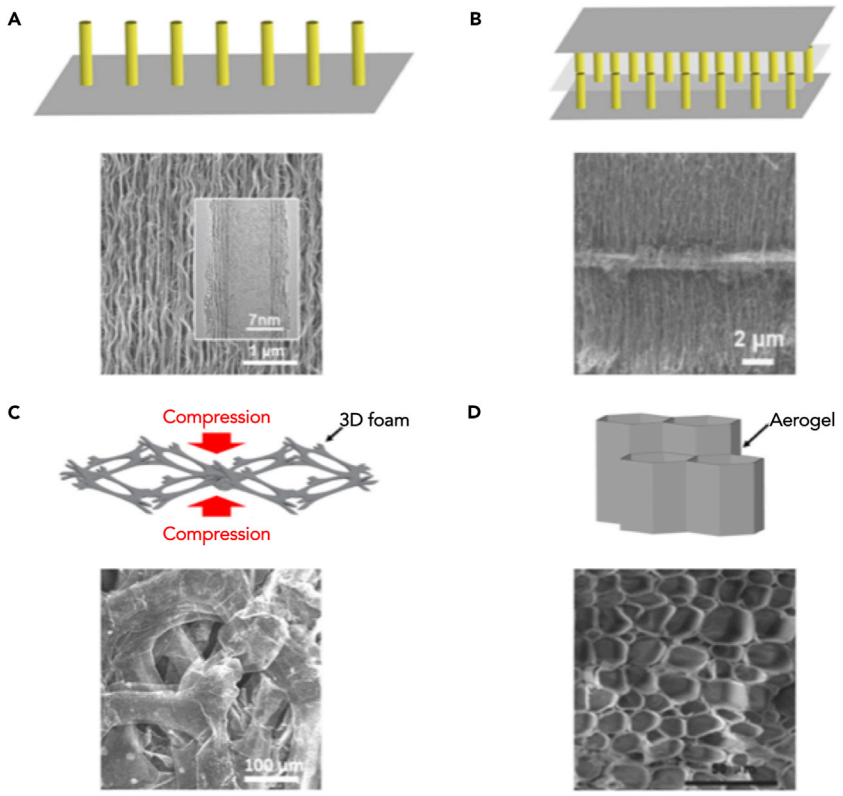

Figure 9. 2D Materials and Their 3D Structure for TIMs

(A–D) Schematic and experimental results are shown at top and bottom of each column separately.

(A) 2D nanosheet with vertically grown 1D nanotubes. Reprinted from Wang et al.,[167] with permission. Copyright 2008, IOP Publishing.

(B) 1D pillared/2D layered structure. Reprinted from Tang et al.,[174] with permission. Copyright 2014, Elsevier.

(C) Compressed 3D foam. Reprinted from Loeblein et al.,[175] with permission. Copyright 2017, American Chemical Society.

(D) Vertically aligned aerogel. Reprinted from Zeng et al.,[162] with permission. Copyright 2015, Wiley.

from satisfactory because of the low thermal conductivity of polymer matrices. On the other hand, using 2D materials as fillers fails to exploit their flexibility. Therefore, directly using 2D materials as thermal management materials has become a pursuit.

3D-Interconnected Graphene and H-BN Macroforms for TIM Applications

Vertically Aligned 1D and 2D Materials. Thermal property research of nanocarbon materials began with vertically aligned carbon nanotubes (VACNTs),[166,167] inspired by their high thermal conductivity of over 3,000 W m^{-1} K^{-1} (Figure 9A).[39] However, thermal resistance between CNT array and Si interface is generally high, because of phonon mismatch between CNTs and Si substrate and the limited number of CNTs contacted with a substrate.[168,169] It has been simulated that a 3D structure made up of CNTs and graphene with covalent bonding would significantly improve cross-plane thermal conductance.[170,171] The concept of pillared structure was proposed in 2008, in which parallel CNTs are used to support graphene sheets as pillars, forming a perpendicular hybrid 3D carbon structure.[172] Although synthesis is a major challenge, a seamless 3D carbon network was produced by CVD, showing covalent bonding between graphene and CNT knots (Figure 9B).[173,174] However, very little research related to their thermal conductance

Please cite this article in press as: Song et al., Two-Dimensional Materials for Thermal Management Applications, Joule (2018), https://doi.org/10.1016/j.joule.2018.01.006

behavior was published, which is partially attributed to the difficulty in thermal conductivity measurements.

Densification of 2D Monoliths. Compression studies show that both compressed 3D graphene and 3D h-BN result in effective enhancement of their cross-plane thermal conductivity. The compression minimizes the pore size but maintains the wall thickness of graphene and h-BN, improving cross-plane thermal conductivity to 62–86 W m^{-1} K^{-1} while keeping its surface conformity (Figure 9C).[175] 3D graphene aerogel by wet chemistry methods also draws great attention. Nevertheless, the pores are usually on the scale of hundreds of micrometers. A compressing procedure is therefore needed to squeeze out the air inside the macroform before the thermal conductivity can be improved (Figure 9D).[162,176]

Graphene and h-BN Thin Films for Heat Spreaders. A heat spreader is used for dissipating heat from a hotspot to its surrounding area. In IC package, it is usually a thin copper or artificial graphite foil with high in-plane thermal conductivity. It has been demonstrated that a mechanically exfoliated few-layer graphene lowers the temperature of a GaN transistor by ~20°C, showing great potential as a heat spreader as well as compatibility with current chip processing.[177] Freestanding reduced graphene oxide (rGO) paper can be fabricated by direct evaporation,[178] vacuum filtration,[179] and electrospray deposition[180] of GO dispersion, as well as surfactant-stabilized graphene nanoplates (GNP) solution.[181] They usually show high thermal conductivity over 1,000 W m^{-1} K^{-1}, outperforming Cu and Al foils in terms of heat spreading capability. Thermal conductivity of the graphene film is effectively dependent on the sheet size of GO[182,183] and its reduction process.[184,185] Kumar et al. fabricated an rGO film by GO sheets with lateral size over 30 μm, showing improved tensile strength (77 MPa) and thermal conductivity (1,390 W m^{-1} K^{-1}) compared with smaller sizes.[186] In a recent work, Peng et al. created microfolds by mechanical pressing of microgasbags between graphene sheets, and these folds provide a graphene paper with mechanical flexibility even after high-temperature annealing (3,000°C). The final graphene paper shows an ultrahigh thermal conductivity of 1,940 W $m^{-1}K^{-1}$,[74] exceeding the best performance of commercially used graphitized polyimide (PI) films.[187]

As graphene films show limited thermal conductivity in the cross-plane direction,[188,189] there have been attempts to build a freestanding 3D connected network to reach the balance between in-plane and cross-plane thermal conductivity.[190] Efforts has been made to increase the thermal conductivity at the cross-plane direction. *In situ* growth of carbon nanoring (CNR) between graphene sheets was reported to form a 3D bridged hybrid paper, and the cross-plane thermal conductivity showed a triple enhancement, reaching 5.8 W m^{-1} K^{-1}.[191] Typical thermal conductivities of graphene-based heat spreaders are summarized in Table 2.

Graphene Fibers for Thermal Management. Graphene fibers can be prepared by wet spinning of concentrated GO dispersion followed by reduction. The outstanding mechanical and electrical properties have made graphene fibers good candidates for versatile applications,[192,193] and the wet-spinning technique makes it easy for mass production up to kilometer scale.[194] For example, Xin et al. fabricated graphene fibers by wet spinning from mixed GO dispersion of large (23 μm) and small (0.8 μm) sheet size. The compact micro-nano hybrid structure enables the fiber to have high tensile strength of 1,080 MPa, achieving a high thermal conductivity of 1,290 W m^{-1} K^{-1} after high-temperature treatments.[195] This is inspiring because lower thermal conductivity is found when using only large-sheet-sized GO at the

Please cite this article in press as: Song et al., Two-Dimensional Materials for Thermal Management Applications, Joule (2018), https://doi.org/10.1016/j.joule.2018.01.006

Table 2. Comparison of Thermal Conductivities of Typical Graphene Films

Materials	K (W m^{-1} K^{-1})	Methods	Reference
rGO	1,100	direct evaporation, 2000°C annealed	Shen et al.[178]
rGO	1,390	vacuum filtration, large GO, hydriodic acid (HI) reduced	Kumar et al.[186]
rGO	1,434	electrospray deposition, 2,850°C annealed	Xin et al.[180]
rGO	1,940	scraping deposition, compressed and 3,000°C annealed	Peng et al.[74]
GNP	1,529	ball milling, 2,850°C annealed	Teng et al.[181]
FLG	1,231 ($\kappa_{\parallel}$) 1.81 ($\kappa_{\perp}$)	Vacuum filtration, functionalized FLG	Liang et al.[179]
rGO + CNR	890 ($\kappa_{\parallel}$) 5.8 ($\kappa_{\perp}$)	Vacuum filtration, *in situ* growth of CNR (800°C)	Zhang et al.[191]
EG + VACNT	255 ($\kappa_{\parallel}$) 35 ($\kappa_{\perp}$)	*in situ* growth of VACNT (850°C)	Qin et al.[190]

EG, expanded graphite; FLG, few-layered graphene.

same concentration, indicating the effectiveness of building the micro-nano hierarchical structure using GO with both large and small sheet sizes at an optimized proportion. It is worth noting that high-temperature annealing can significantly increase thermal conductivity, electrical conductivity, and Young's modulus of graphene. Simultaneously, it has been found that the graphene domain size grows to 780 nm at 2,850°C, which is one order of magnitude higher than that of PAN-based fibers (~20 nm at 2,700°C).[196] The greatly reduced phonon scattering at boundaries facilitates phonon transport and therefore effectively increases thermal conductivity. Further investigations are needed to make graphene fibers fully applicable in thermal management, acting as both fillers and thermal conductive wrappers in flexible devices.

Summary and Outlook

Thermal management has become an emerging topic with the rapid development of electronic and optoelectronic devices. In this review, we have presented an overview of 2D materials with their thermal physics, thermal measurements, and applications in thermal management. Although 2D materials with extraordinary electronic, optical, mechanical, and thermal properties promise numerous opportunities for future electronic, optoelectronic, and other devices, great challenges still exist when using 2D materials for thermal management applications. Here, we outline the three most prominent fields that may lead to breakthroughs in future thermal study and thermal applications of 2D materials.

Understanding Principles of Thermal Physics

2D materials give us a chance to study some fascinating thermal phenomena usually rarely detectable in bulk materials.[197,198] As an example, a recent study discussed the significance of ballistic phonon transport and hydrodynamic phonon transport in graphene,[30] while other studies show the magnitude of ballistic transport in electronic and thermoelectric applications.[199] Moreover, it was calculated in a recent paper that the electronic contribution of thermal conductivity of graphene could be up to ~10%, rather than a negligible value that was widely accepted previously.[200] However, definitive experimental data supporting such a perspective is still lacking. In addition, it is widely accepted that an enhanced interfacial coupling would increase interface thermal conductance,[63] while precise measurements of interface thermal conductance are still a challenge, especially for atomically thick

Please cite this article in press as: Song et al., Two-Dimensional Materials for Thermal Management Applications, Joule (2018), https://doi.org/10.1016/j.joule.2018.01.006

van der Waals heterostructures.[201] A recent study proved that the solubility parameter may be the dominant factor for interface thermal conductance, the in-depth study of which may give clues on designing thermal interface and open a new avenue of understanding and controlling of heat flux in 2D materials and next-generation electronic devices.[202]

Controlled Growth and Assembly of 2D Materials into Designed Macrostructures

2D materials can be viewed as building blocks for assembly into 2D structures. Depending on the ways of assembly, different 3D macrostructures (i.e., thin films, foams, or 3D monoliths with defined structures) are useful in various thermal applications depending on heat dissipation requirements. In achieving maximum enhancement of thermal properties using 2D materials as TIM fillers, the construction of phonon conduits and growth of large domains of 2D materials are of great importance, as thermal conductivity is largely dependent on thermal percolation threshold and crystal domain sizes. In addition, 2D materials can be directly used as heat spreaders, for which controlled growth of 2D materials with preferable assembly on electronic devices is required. Vertically aligned graphene and CNT have shed light on the problem of c-axis thermal conductance; however, the thermal contact resistance between individual graphene flake and CNT is always a concern, which limits the performance in thermal management applications.[203,204] Meanwhile, low-temperature CVD growth of graphene and h-BN on polymer substrate is always a popular topic for flexible electronic devices.[205] Innovations in growing customized structures of 2D materials and their 3D macroforms within the specific context of application are much needed to develop thermal management applications for next-generation electronic devices.

Improving Thermal Measurement Methods

Despite great progress on measuring thermal properties of 2D nanomaterials, there are still questions that remain to be answered. Thermal conductivity data of samples with identical thickness may differ significantly from each other, varying from measurement to measurement and from sample to sample, which is not surprising because lateral sizes and environment of samples may also play an important role while it is difficult to precisely measure and control them.[90] It is still hoped that a novel thermal measurement method with lower errors of data and better adaptability to samples could be developed, with which researchers would be able to have a better understanding of fundamental thermal physics and a stronger tool to design thermal management applications.

ACKNOWLEDGMENTS

The authors acknowledge the financial support from National Natural Science Foundation of China (nos. 51521091 and 51722206), Shenzhen Municipal Development and Reform Commission, Shenzhen Environmental Science and New Energy Technology Engineering Laboratory grant number: SDRC [2016]172, the Youth 1000-Talent Program of China, the Shenzhen Basic Research Project (no. JCYJ20170307140956657), and the Development and Reform Commission of Shenzhen Municipality for the development of the "Low-Dimensional Materials and Devices" Discipline.

AUTHOR CONTRIBUTIONS

H.-M.C. and F.K. proposed the topic of this review. H.S. and J.L. investigated the literature and wrote the manuscript. J.W. and B.L. revised the manuscript.

REFERENCES

1. Song, Y.M., Xie, Y., Malyarchuk, V., Xiao, J., Jung, I., Choi, K.J., Liu, Z., Park, H., Lu, C., and Kim, R.H. (2013). Digital cameras with designs inspired by the arthropod eye. Nature *497*, 95–99.
2. Bauer, S. (2013). Flexible electronics: sophisticated skin. Nat. Mater. *12*, 871–872.
3. Thompson, S.E., and Parthasarathy, S. (2006). Moore's law: the future of Si microelectronics. Mater. Today *9*, 20–25.
4. Intel 50 Years of Moore's Law. https://www.intel.com/content/www/us/en/silicon-innovations/moores-law-technology.html.
5. Hamann, H.F., Weger, A., Lacey, J.A., Hu, Z., Bose, P., Cohen, E., and Wakil, J. (2007). Hotspot-limited microprocessors: direct temperature and power distribution measurements. IEEE J. Solid State Circuits *42*, 56–65.
6. Pop, E. (2010). Energy dissipation and transport in nanoscale devices. Nano Res. *3*, 147–169.
7. Balandin, A.A. (2011). Thermal properties of graphene and nanostructured carbon materials. Nat. Mater. *10*, 569–581.
8. Nika, D.L., and Balandin, A.A. (2012). Two-dimensional phonon transport in graphene. J. Phys. Condens. Matter *24*, 233203.
9. Novoselov, K.S., Geim, A.K., Morozov, S.V., Jiang, D., Zhang, Y., Dubonos, S.V., Grigorieva, I.V., and Firsov, A.A. (2004). Electric field effect in atomically thin carbon films. Science *306*, 666–669.
10. Golberg, D., Bando, Y., Huang, Y., Terao, T., Mitome, M., Tang, C., and Zhi, C. (2010). Boron nitride nanotubes and nanosheets. ACS Nano *4*, 2979–2993.
11. Radisavljevic, B., Radenovic, A., Brivio, J., Giacometti, V., and Kis, A. (2011). Single-layer MoS_2 transistors. Nat. Nanotechnol. *6*, 147–150.
12. Liu, B., Köpf, M., Abbas, A.N., Wang, X., Guo, Q., Jia, Y., Xia, F., Weihrich, R., Bachhuber, F., and Pielnhofer, F. (2015). Black arsenic-phosphorus: layered anisotropic infrared semiconductors with highly tunable compositions and properties. Adv. Mater. *27*, 4423–4429.
13. Lin, Y.M., Dimitrakopoulos, C., Jenkins, K.A., Farmer, D.B., Chiu, H.Y., Grill, A., and Avouris, P. (2010). 100-GHz transistors from wafer-scale epitaxial graphene. Science *327*, 662.
14. Mueller, T., Xia, F., and Avouris, P. (2010). Graphene photodetectors for high-speed optical communications. Nat. Photon. *4*, 297–301.
15. Pospischil, A., Furchi, M.M., and Mueller, T. (2014). Solar-energy conversion and light emission in an atomic monolayer pn diode. Nat. Nanotechnol. *9*, 257–261.
16. Yang, X., Cheng, C., Wang, Y., Qiu, L., and Li, D. (2013). Liquid-mediated dense integration of graphene materials for compact capacitive energy storage. Science *341*, 534–537.
17. Li, Y., Wang, H., Xie, L., Liang, Y., Hong, G., and Dai, H. (2011). MoS2 nanoparticles grown on graphene: an advanced catalyst for the hydrogen evolution reaction. J. Am. Chem. Soc. *133*, 7296–7299.
18. Liu, B., Chen, L., Liu, G., Abbas, A.N., Fathi, M., and Zhou, C. (2014). High-performance chemical sensing using Schottky-contacted chemical vapor deposition grown monolayer MoS_2 transistors. ACS Nano *8*, 5304–5314.
19. Ghosh, S., Calizo, I., Teweldebrhan, D., Pokatilov, E.P., Nika, D.L., Balandin, A.A., Bao, W., Miao, F., and Lau, C.N. (2008). Extremely high thermal conductivity of graphene: prospects for thermal management applications in nanoelectronic circuits. Appl. Phys. Lett. *92*, 151911.
20. Lui, C.H., Liu, L., Mak, K.F., Flynn, G.W., and Heinz, T.F. (2009). Ultraflat graphene. Nature *462*, 339–341.
21. Schwierz, F. (2010). Graphene transistors. Nat. Nanotechnol. *5*, 487–496.
22. Balandin, A.A., Ghosh, S., Bao, W., Calizo, I., Teweldebrhan, D., Miao, F., and Lau, C.N. (2008). Superior thermal conductivity of single-layer graphene. Nano Lett. *8*, 902–907.
23. Nika, D.L., Pokatilov, E.P., and Balandin, A.A. (2011). Theoretical description of thermal transport in graphene: the issues of phonon cut-off frequencies and polarization branches. Phys. Status Solidi B *248*, 2609–2614.
24. Touloukian, Y.S., ed. (1970). In Thermophysical properties of matter: the TPRC data series; a comprehensive compilation of data, *Volume 6* (Ifi/Plenum), p. 1.
25. Malekpour, H., Chang, K.H., Chen, J.C., Lu, C.Y., Nika, D., Novoselov, K., and Balandin, A. (2014). Thermal conductivity of graphene laminate. Nano Lett. *14*, 5155–5161.
26. Goli, P., Ning, H., Li, X., Lu, C.Y., Novoselov, K.S., and Balandin, A.A. (2014). Thermal properties of graphene-copper-graphene heterogeneous films. Nano Lett. *14*, 1497–1503.
27. Zhi, C., Bando, Y., Tang, C., Kuwahara, H., and Golberg, D. (2009). Large-scale fabrication of boron nitride nanosheets and their utilization in polymeric composites with improved thermal and mechanical properties. Adv. Mater. *21*, 2889–2893.
28. Shaikh, S., Li, L., Lafdi, K., and Huie, J. (2007). Thermal conductivity of an aligned carbon nanotube array. Carbon *45*, 2608–2613.
29. Hu, Y., Zeng, L., Minnich, A.J., Dresselhaus, M.S., and Chen, G. (2015). Spectral mapping of thermal conductivity through nanoscale ballistic transport. Nat. Nanotechnol. *10*, 701–706.
30. Lee, S., Broido, D., Esfarjani, K., and Chen, G. (2015). Hydrodynamic phonon transport in suspended graphene. Nat. Commun. *6*, 6290.
31. Wang, Y., Xu, N., Li, D., and Zhu, J. (2017). Thermal properties of two dimensional layered materials. Adv. Funct. Mater. *27*, https://doi.org/10.1002/adfm.201604134.
32. Renteria, J.D., Nika, D.L., and Balandin, A.A. (2014). Graphene thermal properties: applications in thermal management and energy storage. Appl. Sci. *4*, 525–547.
33. Yan, Z., Nika, D.L., and Balandin, A.A. (2015). Thermal properties of graphene and few-layer graphene: applications in electronics. IET Circuits Devices Syst. *9*, 4–12.
34. Carslaw, H.S., and Jaeger, J.C. (1959). Conduction of Heat in Solids, Second Edition (Clarendon Press).
35. Nika, D., Pokatilov, E., Askerov, A., and Balandin, A. (2009). Phonon thermal conduction in graphene: role of Umklapp and edge roughness scattering. Phys. Rev. B *79*, 155413.
36. Klemens, P. (1958). Thermal conductivity and lattice vibrational modes. Solid State Phys. *7*, 1–98.
37. Swartz, E.T., and Pohl, R.O. (1989). Thermal boundary resistance. Rev. Mod. Phys. *61*, 605.
38. Hu, J., Ruan, X., and Chen, Y.P. (2009). Thermal conductivity and thermal rectification in graphene nanoribbons: a molecular dynamics study. Nano Lett. *9*, 2730–2735.
39. Kim, P., Shi, L., Majumdar, A., and McEuen, P. (2001). Thermal transport measurements of individual multiwalled nanotubes. Phys. Rev. Lett. *87*, 215502.
40. Cahill, D.G. (1990). Thermal conductivity measurement from 30 to 750 K: the 3ω method. Rev. Sci. Instrum. *61*, 802–808.
41. Paddock, C.A., and Eesley, G.L. (1986). Transient thermoreflectance from thin metal films. J. Appl. Phys. *60*, 285–290.
42. Nika, D.L., and Balandin, A.A. (2017). Phonons and thermal transport in graphene and graphene-based materials. Rep. Prog. Phys. *80*, 036502.
43. Calizo, I., Balandin, A., Bao, W., Miao, F., and Lau, C. (2007). Temperature dependence of the Raman spectra of graphene and graphene multilayers. Nano Lett. *7*, 2645–2649.
44. Cai, W., Moore, A.L., Zhu, Y., Li, X., Chen, S., Shi, L., and Ruoff, R.S. (2010). Thermal transport in suspended and supported monolayer graphene grown by chemical vapor deposition. Nano Lett. *10*, 1645–1651.
45. Faugeras, C., Faugeras, B., Orlita, M., Potemski, M., Nair, R.R., and Geim, A. (2010). Thermal conductivity of graphene in corbino membrane geometry. ACS Nano *4*, 1889–1892.
46. Zhou, H., Zhu, J., Liu, Z., Yan, Z., Fan, X., Lin, J., Wang, G., Yan, Q., Yu, T., Ajayan, P.M., and Tour, J.M. (2014). High thermal conductivity of suspended few-layer hexagonal boron nitride sheets. Nano Res. *7*, 1232–1240.
47. Sahoo, S., Gaur, A.P., Ahmadi, M., Guinel, M.J.F., and Katiyar, R.S. (2013). Temperature-dependent Raman studies and thermal conductivity of few-layer MoS_2. J. Phys. Chem. C *117*, 9042–9047.

48. Yan, R., Simpson, J.R., Bertolazzi, S., Brivio, J., Watson, M., Wu, X., Kis, A., Luo, T., Hight Walker, A.R., and Xing, H.G. (2014). Thermal conductivity of monolayer molybdenum disulfide obtained from temperature-dependent Raman spectroscopy. ACS Nano *8*, 986–993.

49. Peimyoo, N., Shang, J., Yang, W., Wang, Y., Cong, C., and Yu, T. (2015). Thermal conductivity determination of suspended mono-and bilayer WS2 by Raman spectroscopy. Nano Res. *8*, 1210–1221.

50. Chen, S., Moore, A.L., Cai, W., Suk, J.W., An, J., Mishra, C., Amos, C., Magnuson, C.W., Kang, J., Shi, L., and Ruoff, R.S. (2011). Raman measurements of thermal transport in suspended monolayer graphene of variable sizes in vacuum and gaseous environments. ACS Nano *5*, 321–328.

51. Jo, I., Pettes, M.T., Kim, J., Watanabe, K., Taniguchi, T., Yao, Z., and Shi, L. (2013). Thermal conductivity and phonon transport in suspended few-layer hexagonal boron nitride. Nano Lett. *13*, 550–554.

52. Seol, J.H., Jo, I., Moore, A.L., Lindsay, L., Aitken, Z.H., Pettes, M.T., Li, X., Yao, Z., Huang, R., Broido, D., et al. (2010). Two-dimensional phonon transport in supported graphene. Science *328*, 213–216.

53. Xu, X., Pereira, L.F., Wang, Y., Wu, J., Zhang, K., Zhao, X., Bae, S., Bui, C.T., Xie, R., Thong, J.T., et al. (2014). Length-dependent thermal conductivity in suspended single-layer graphene. Nat. Commun. *5*, 1–6.

54. Jo, I., Pettes, M.T., Ou, E., Wu, W., and Shi, L. (2014). Basal-plane thermal conductivity of few-layer molybdenum disulfide. Appl. Phys. Lett. *104*, 201902.

55. Lee, S., Yang, F., Suh, J., Yang, S., Lee, Y., Li, G., Choe, H.S., Suslu, A., Chen, Y., and Ko, C. (2015). Anisotropic in-plane thermal conductivity of black phosphorus nanoribbons at temperatures higher than 100 K. Nat. Commun. *6*, https://doi.org/10.1038/ncomms9573.

56. Pettes, M.T., Maassen, J., Jo, I., Lundstrom, M.S., and Shi, L. (2013). Effects of surface band bending and scattering on thermoelectric transport in suspended bismuth telluride nanoplates. Nano Lett. *13*, 5316–5322.

57. Sadeghi, M.M., Pettes, M.T., and Shi, L. (2012). Thermal transport in graphene. Solid State Commun. *152*, 1321–1330.

58. Pettes, M.T., Jo, I., Yao, Z., and Shi, L. (2011). Influence of polymeric residue on the thermal conductivity of suspended bilayer graphene. Nano Lett. *11*, 1195–1200.

59. Wang, Z., Xie, R., Bui, C.T., Liu, D., Ni, X., Li, B., and Thong, J.T. (2010). Thermal transport in suspended and supported few-layer graphene. Nano Lett. *11*, 113–118.

60. Schmidt, A.J., Chen, X., and Chen, G. (2008). Pulse accumulation, radial heat conduction, and anisotropic thermal conductivity in pump-probe transient thermoreflectance. Rev. Sci. Instrum. *79*, 114902.

61. Cahill, D.G. (2004). Analysis of heat flow in layered structures for time-domain thermoreflectance. Rev. Sci. Instrum. *75*, 5119–5122.

62. Costescu, R.M., Wall, M.A., and Cahill, D.G. (2003). Thermal conductance of epitaxial interfaces. Phys. Rev. B *67*, 054302.

63. Losego, M.D., Grady, M.E., Sottos, N.R., Cahill, D.G., and Braun, P.V. (2012). Effects of chemical bonding on heat transport across interfaces. Nat. Mater. *11*, 502–506.

64. Hopkins, P.E., Baraket, M., Barnat, E.V., Beechem, T.E., Kearney, S.P., Duda, J.C., Robinson, J.T., and Walton, S.G. (2012). Manipulating thermal conductance at metal-graphene contacts via chemical functionalization. Nano Lett. *12*, 590–595.

65. Zhang, C., Chen, W., Tao, Y., Zhao, W., Cai, S., Liu, C., Ni, Z., Xu, D., Wei, Z., and Yang, J. (2017). Electron contributions to the heat conduction across Au/graphene/Au interfaces. Carbon *115*, 665–671.

66. Schmidt, A.J., Collins, K.C., Minnich, A.J., and Chen, G. (2010). Thermal conductance and phonon transmissivity of metal-graphite interfaces. J. Appl. Phys. *107*, 104907.

67. Jiang, T., Zhang, X., Vishwanath, S., Mu, X., Kanzyuba, V., Sokolov, D.A., Ptasinska, S., Go, D.B., Xing, H.G., and Luo, T. (2016). Covalent bonding modulated graphene-metal interfacial thermal transport. Nanoscale *8*, 10993–11001.

68. Koh, Y.K., Bae, M.H., Cahill, D.G., and Pop, E. (2010). Heat conduction across monolayer and few-layer graphenes. Nano Lett. *10*, 4363–4368.

69. Jang, H., Wood, J.D., Ryder, C.R., Hersam, M.C., and Cahill, D.G. (2015). Anisotropic thermal conductivity of exfoliated black phosphorus. Adv. Mater. *27*, 8017–8022.

70. Chiritescu, C., Cahill, D.G., Nguyen, N., Johnson, D., Bodapati, A., Keblinski, P., and Zschack, P. (2007). Ultralow thermal conductivity in disordered, layered WSe_2 crystals. Science *315*, 351.

71. Shi, L., Plyasunov, S., Bachtold, A., McEuen, P.L., and Majumdar, A. (2000). Scanning thermal microscopy of carbon nanotubes using batch-fabricated probes. Appl. Phys. Lett. *77*, 4295–4297.

72. Kim, K., Chung, J., Hwang, G., Kwon, O., and Lee, J.S. (2011). Quantitative measurement with scanning thermal microscope by preventing the distortion due to the heat transfer through the air. ACS Nano *5*, 8700–8709.

73. Yoon, K., Hwang, G., Chung, J., goo Kim, H., Kwon, O., Kihm, K.D., and Lee, J.S. (2014). Measuring the thermal conductivity of residue-free suspended graphene bridge using null point scanning thermal microscopy. Carbon *76*, 77–83.

74. Peng, L., Xu, Z., Liu, Z., Guo, Y., Li, P., and Gao, C. (2017). Ultrahigh thermal conductive yet superflexible graphene films. Adv. Mater. *29*, https://doi.org/10.1002/adma.201700589.

75. Klemens, P. (2000). Theory of the a-plane thermal conductivity of graphite. J. Wide Bandgap Mater. *7*, 332–339.

76. Slack, G.A. (1962). Anisotropic thermal conductivity of pyrolytic graphite. Phys. Rev. *127*, 694.

77. Xu, Y., Chen, X., Gu, B.-L., and Duan, W. (2009). Intrinsic anisotropy of thermal conductance in graphene nanoribbons. Appl. Phys. Lett. *95*, 233116.

78. Wei, Z., Chen, Y., and Dames, C. (2012). Wave packet simulations of phonon boundary scattering at graphene edges. J. Appl. Phys. *112*, 024328.

79. Luo, Z., Maassen, J., Deng, Y., Du, Y., Garrelts, R.P., Lundstrom, M.S., Peide, D.Y., and Xu, X. (2015). Anisotropic in-plane thermal conductivity observed in few-layer black phosphorus. Nat. Commun. *6*, 8572.

80. Klemens, P., and Pedraza, D. (1994). Thermal conductivity of graphite in the basal plane. Carbon *32*, 735–741.

81. Null, M., Lozier, W., and Moore, A. (1973). Thermal diffusivity and thermal conductivity of pyrolytic graphite from 300 to 2700 K. Carbon *11*, 81–87.

82. Mounet, N., and Marzari, N. (2005). First-principles determination of the structural, vibrational and thermodynamic properties of diamond, graphite, and derivatives. Phys. Rev. B *71*, 205214.

83. Lindsay, L., Broido, D.A., and Mingo, N. (2010). Flexural phonons and thermal transport in graphene. Phys. Rev. B *82*, 1537–1546.

84. Lindsay, L., Broido, D., and Mingo, N. (2010). Diameter dependence of carbon nanotube thermal conductivity and extension to the graphene limit. Phys. Rev. B *82*, 161402.

85. Lindsay, L., Li, W., Carrete, J., Mingo, N., Broido, D.A., and Reinecke, T.L. (2014). Phonon thermal transport in strained and unstrained graphene from first principles. Phys. Rev. B *89*, 1537–1538.

86. Ghosh, S., Bao, W., Nika, D.L., Subrina, S., Pokatilov, E.P., Lau, C.N., and Balandin, A.A. (2010). Dimensional crossover of thermal transport in few-layer graphene. Nat. Mater. *9*, 555–558.

87. Sadeghi, M.M., Jo, I., and Shi, L. (2013). Phonon-interface scattering in multilayer graphene on an amorphous support. Proc. Natl. Acad. Sci. USA *110*, 16321–16326.

88. Lee, J.-U., Yoon, D., Kim, H., Lee, S.W., and Cheong, H. (2011). Thermal conductivity of suspended pristine graphene measured by Raman spectroscopy. Phys. Rev. B *83*, 081419.

89. Nika, D., Ghosh, S., Pokatilov, E., and Balandin, A. (2009). Lattice thermal conductivity of graphene flakes: comparison with bulk graphite. Appl. Phys. Lett. *94*, 203103.

90. Nika, D.L., Askerov, A.S., and Balandin, A.A. (2012). Anomalous size dependence of the thermal conductivity of graphene ribbons. Nano Lett. *12*, 3238–3244.

91. Fthenakis, Z.G., Zhu, Z., and Tománek, D. (2014). Effect of structural defects on the thermal conductivity of graphene: from point

to line defects to haeckelites. Phys. Rev. B *89*, 125421.

92. Ma, T., Liu, Z., Wen, J., Gao, Y., Ren, X., Chen, H., Jin, C., Ma, X.L., Xu, N., Cheng, H.M., and Ren, W. (2017). Tailoring the thermal and electrical transport properties of graphene films by grain size engineering. Nat. Commun. *8*, 1–9.

93. Novoselov, K., Mishchenko, A., Carvalho, A., and Neto, A.C. (2016). 2D materials and van der Waals heterostructures. Science *353*, aac9439.

94. Liu, Z., Ma, L., Shi, G., Zhou, W., Gong, Y., Lei, S., Yang, X., Zhang, J., Yu, J., and Hackenberg, K.P. (2013). In-plane heterostructures of graphene and hexagonal boron nitride with controlled domain sizes. Nat. Nanotechnol. *8*, 119–124.

95. Britnell, L., Gorbachev, R., Jalil, R., Belle, B., Schedin, F., Mishchenko, A., Georgiou, T., Katsnelson, M., Eaves, L., and Morozov, S. (2012). Field-effect tunneling transistor based on vertical graphene heterostructures. Science *335*, 947–950.

96. Dean, C.R., Young, A.F., Meric, I., Lee, C., Wang, L., Sorgenfrei, S., Watanabe, K., Taniguchi, T., Kim, P., and Shepard, K.L. (2010). Boron nitride substrates for high-quality graphene electronics. Nat. Nanotechnol. *5*, 722–726.

97. Jin, C., Kim, J., Suh, J., Shi, Z., Chen, B., Fan, X., Kam, M., Watanabe, K., Taniguchi, T., and Tongay, S. (2017). Interlayer electron-phonon coupling in WSe_2/hBN heterostructures. Nat. Phys. *13*, 127–131.

98. Zou, J.-H., and Cao, B.-Y. (2017). Phonon thermal properties of graphene on h-BN from molecular dynamics simulations. Appl. Phys. Lett. *110*, 103106.

99. Liu, Y., Ong, Z.Y., Wu, J., Zhao, Y., Watanabe, K., Taniguchi, T., Chi, D., Zhang, G., Thong, J.T., and Qiu, C.W. (2017). Thermal conductance of the 2D MoS_2/h-BN and graphene/h-BN interfaces. Sci. Rep. *7*, 43886.

100. Mak, K.F., Lui, C.H., and Heinz, T.F. (2010). Measurement of the thermal conductance of the graphene/SiO_2 interface. Appl. Phys. Lett. *97*, 221904.

101. Chen, Z., Jang, W., Bao, W., Lau, C., and Dames, C. (2009). Thermal contact resistance between graphene and silicon dioxide. Appl. Phys. Lett. *95*, 161910.

102. Sachs, B., Wehling, T., Katsnelson, M., and Lichtenstein, A. (2011). Adhesion and electronic structure of graphene on hexagonal boron nitride substrates. Phys. Rev. B *84*, 195414.

103. Yan, Z., Chen, L., Yoon, M., and Kumar, S. (2016). Phonon transport at the interfaces of vertically stacked graphene and hexagonal boron nitride heterostructures. Nanoscale *8*, 4037–4046.

104. Liu, X., Zhang, G., and Zhang, Y.W. (2016). Topological defects at the graphene/h-BN interface abnormally enhance its thermal conductance. Nano Lett. *16*, 4954–4959.

105. Chen, S., Wu, Q., Mishra, C., Kang, J., Zhang, H., Cho, K., Cai, W., Balandin, A.A., and Ruoff, R.S. (2012). Thermal conductivity of isotopically modified graphene. Nat. Mater. *11*, 203–207.

106. Zhu, G., Liu, J., Zheng, Q., Zhang, R., Li, D., Banerjee, D., and Cahill, D.G. (2016). Tuning thermal conductivity in molybdenum disulfide by electrochemical intercalation. Nat. Commun. *7*, https://doi.org/10.1038/ncomms13211.

107. Bonini, N., Garg, J., and Marzari, N. (2012). Acoustic phonon lifetimes and thermal transport in free-standing and strained graphene. Nano Lett. *12*, 2673–2678.

108. Hao, F., Fang, D., and Xu, Z. (2011). Mechanical and thermal transport properties of graphene with defects. Appl. Phys. Lett. *99*, 041901.

109. Kim, J.Y., Lee, J.H., and Grossman, J.C. (2012). Thermal transport in functionalized graphene. ACS Nano *6*, 9050–9057.

110. Tong, X.C. (2011). Advanced Materials for Thermal Management of Electronic Packaging, *Vol. 30* (Springer Science & Business Media).

111. Wang, Q., Xia, H., and Zhang, C. (2001). Preparation of polymer/inorganic nanoparticles composites through ultrasonic irradiation. J. Appl. Polym. Sci. *80*, 1478–1488.

112. Kozako, M., Okazaki, Y., Hikita, M., and Tanaka, T. (2010). Preparation and evaluation of epoxy composite insulating materials toward high thermal conductivity. Solid Dielectrics (ICSD), 2010 10th IEEE International Conference (IEEE), pp. 1–4.

113. Yu, S., Hing, P., and Hu, X. (2002). Thermal conductivity of polystyrene–aluminum nitride composite. Compos. Part A Appl. Sci. Manuf. *33*, 289–292.

114. Yujun, G., Zhongliang, L., Guangmeng, Z., and Yanxia, L. (2014). Effects of multi-walled carbon nanotubes addition on thermal properties of thermal grease. Int. J. Heat Mass Transf. *74*, 358–367.

115. Yu, A., Ramesh, P., Itkis, M.E., Bekyarova, E., and Haddon, R.C. (2007). Graphite nanoplatelet-epoxy composite thermal interface materials. J. Phys. Chem. C *111*, 7565–7569.

116. Pashayi, K., Fard, H.R., Lai, F., Iruvanti, S., Plawsky, J., and Borca-Tasciuc, T. (2012). High thermal conductivity epoxy-silver composites based on self-constructed nanostructured metallic networks. J. Appl. Phys. *111*, 104310.

117. Chen, H., Ginzburg, V.V., Yang, J., Yang, Y., Liu, W., Huang, Y., Du, L., and Chen, B. (2016). Thermal conductivity of polymer-based composites: fundamentals and applications. Prog. Polym. Sci. *59*, 41–85.

118. Yu, A., Ramesh, P., Sun, X., Bekyarova, E., Itkis, M.E., and Haddon, R.C. (2008). Enhanced thermal conductivity in a hybrid graphite nanoplatelet-carbon nanotube filler for epoxy composites. Adv. Mater. *20*, 4740–4744.

119. Shahil, K.M., and Balandin, A.A. (2012). Graphene–multilayer graphene nanocomposites as highly efficient thermal interface materials. Nano Lett. *12*, 861–867.

120. Teng, C.-C., Ma, C.-C.M., Lu, C.-H., Yang, S.-Y., Lee, S.-H., Hsiao, M.-C., Yen, M.-Y., Chiou, K.-C., and Lee, T.-M. (2011). Thermal conductivity and structure of non-covalent functionalized graphene/epoxy composites. Carbon *49*, 5107–5116.

121. Li, T.L., and Hsu, S.L. (2010). Enhanced thermal conductivity of polyimide films via a hybrid of micro- and nano-sized boron nitride. J. Phys. Chem. B *114*, 6825–6829.

122. Song, W.L., Wang, P., Cao, L., Anderson, A., Meziani, M.J., Farr, A.J., and Sun, Y.P. (2012). Polymer/boron nitride nanocomposite materials for superior thermal transport performance. Angew. Chem. Int. Ed. *51*, 6498–6501.

123. Huang, X., Zhi, C., Jiang, P., Golberg, D., Bando, Y., and Tanaka, T. (2013). Polyhedral oligosilsesquioxane-modified boron nitride nanotube based epoxy nanocomposites: an ideal dielectric material with high thermal conductivity. Adv. Funct. Mater. *23*, 1824–1831.

124. Goli, P., Legedza, S., Dhar, A., Salgado, R., Renteria, J., and Balandin, A.A. (2014). Graphene-enhanced hybrid phase change materials for thermal management of Li-ion batteries. J. Power Source *248*, 37–43.

125. Renteria, J., Legedza, S., Salgado, R., Balandin, M., Ramirez, S., Saadah, M., Kargar, F., and Balandin, A. (2015). Magnetically-functionalized self-aligning graphene fillers for high-efficiency thermal management applications. Mater. Des. *88*, 214–221.

126. Saadah, M., Hernandez, E., and Balandin, A.A. (2017). Thermal management of concentrated multi-junction solar cells with graphene-enhanced thermal interface materials. Appl. Sci. *7*, 589.

127. Bigg, D. (1986). Thermally conductive polymer compositions. Polym. Compos. *7*, 125–140.

128. Stankovich, S., Dikin, D.A., Piner, R.D., Kohlhaas, K.A., Kleinhammes, A., Jia, Y., Wu, Y., Nguyen, S.T., and Ruoff, R.S. (2007). Synthesis of graphene-based nanosheets via chemical reduction of exfoliated graphite oxide. Carbon *45*, 1558–1565.

129. Marcano, D.C., Kosynkin, D.V., Berlin, J.M., Sinitskii, A., Sun, Z., Slesarev, A., Alemany, L.B., Lu, W., and Tour, J.M. (2010). Improved synthesis of graphene oxide. ACS Nano *4*, 4806–4814.

130. Lei, W., Mochalin, V.N., Liu, D., Qin, S., Gogotsi, Y., and Chen, Y. (2015). Boron nitride colloidal solutions, ultralight aerogels and freestanding membranes through one-step exfoliation and functionalization. Nat. Commun. *6*, 8849.

131. Sainsbury, T., Satti, A., May, P., Wang, Z., McGovern, I., Gun'ko, Y.K., and Coleman, J. (2012). Oxygen radical functionalization of boron nitride nanosheets. J. Am. Chem. Soc. *134*, 18758–18771.

132. Nicolosi, V., Chhowalla, M., Kanatzidis, M.G., Strano, M.S., and Coleman, J.N. (2013). Liquid exfoliation of layered materials. Science *340*, 1226419.

133. Shih, C.J., Vijayaraghavan, A., Krishnan, R., Sharma, R., Han, J.H., Ham, M.H., Jin, Z., Lin,

S., Paulus, G.L., and Reuel, N.F. (2011). Bi- and trilayer graphene solutions. Nat. Nanotechnol. *6*, 439–445.

134. Hernandez, Y., Nicolosi, V., Lotya, M., Blighe, F.M., Sun, Z., De, S., McGovern, I., Holland, B., Byrne, M., and Gun'Ko, Y.K. (2008). High-yield production of graphene by liquid-phase exfoliation of graphite. Nat. Nanotechnol. *3*, 563–568.

135. Lotya, M., Hernandez, Y., King, P.J., Smith, R.J., Nicolosi, V., Karlsson, L.S., Blighe, F.M., De, S., Wang, Z., and McGovern, I. (2009). Liquid phase production of graphene by exfoliation of graphite in surfactant/water solutions. J. Am. Chem. Soc. *131*, 3611–3620.

136. Coleman, J.N., Lotya, M., O'Neill, A., Bergin, S.D., King, P.J., Khan, U., Young, K., Gaucher, A., De, S., and Smith, R.J. (2011). Two-dimensional nanosheets produced by liquid exfoliation of layered materials. Science *331*, 568–571.

137. Song, Y.S., and Youn, J.R. (2005). Influence of dispersion states of carbon nanotubes on physical properties of epoxy nanocomposites. Carbon *43*, 1378–1385.

138. Tang, L.-C., Wan, Y.-J., Yan, D., Pei, Y.-B., Zhao, L., Li, Y.-B., Wu, L.-B., Jiang, J.-X., and Lai, G.-Q. (2013). The effect of graphene dispersion on the mechanical properties of graphene/epoxy composites. Carbon *60*, 16–27.

139. Choi, S., Im, H., and Kim, J. (2012). Flexible and high thermal conductivity thin films based on polymer: aminated multi-walled carbon nanotubes/micro-aluminum nitride hybrid composites. Compos. Part A Appl. Sci. Manuf. *43*, 1860–1868.

140. Ganguli, S., Roy, A.K., and Anderson, D.P. (2008). Improved thermal conductivity for chemically functionalized exfoliated graphite/epoxy composites. Carbon *46*, 806–817.

141. Lee, H.-J., Han, S.-W., Kwon, Y.-D., Tan, L.-S., and Baek, J.-B. (2008). Functionalization of multi-walled carbon nanotubes with various 4-substituted benzoic acids in mild polyphosphoric acid/phosphorous pentoxide. Carbon *46*, 1850–1859.

142. Gulotty, R., Castellino, M., Jagdale, P., Tagliaferro, A., and Balandin, A.A. (2013). Effects of functionalization on thermal properties of single-wall and multi-wall carbon nanotube–polymer nanocomposites. ACS Nano *7*, 5114–5121.

143. Song, S.H., Park, K.H., Kim, B.H., Choi, Y.W., Jun, G.H., Lee, D.J., Kong, B.S., Paik, K.W., and Jeon, S. (2013). Enhanced thermal conductivity of epoxy-graphene composites by using non-oxidized graphene flakes with non-covalent functionalization. Adv. Mater. *25*, 732–737.

144. Dreyer, D.R., Park, S., Bielawski, C.W., and Ruoff, R.S. (2010). The chemistry of graphene oxide. Chem. Soc. Rev. *39*, 228–240.

145. Huang, X., Qi, X., Boey, F., and Zhang, H. (2012). Graphene-based composites. Chem. Soc. Rev. *41*, 666–686.

146. Huang, X., Zhi, C., and Jiang, P. (2012). Toward effective synergetic effects from graphene nanoplatelets and carbon nanotubes on thermal conductivity of ultrahigh volume fraction nanocarbon epoxy composites. J. Phys. Chem. C *116*, 23812–23820.

147. Zeng, X., Ye, L., Yu, S., Li, H., Sun, R., Xu, J., and Wong, C.P. (2015). Artificial nacre-like papers based on noncovalent functionalized boron nitride nanosheets with excellent mechanical and thermally conductive properties. Nanoscale *7*, 6774–6781.

148. Yao, Y., Zeng, X., Sun, R., Xu, J.B., and Wong, C.P. (2016). Highly thermally conductive composite papers prepared based on the thought of bioinspired engineering. ACS Appl. Mater. Inter. *8*, 15645–15653.

149. Ding, P., Zhang, J., Song, N., Tang, S., Liu, Y., and Shi, L. (2015). Anisotropic thermal conductive properties of hot-pressed polystyrene/graphene composites in the through-plane and in-plane directions. Compos. Sci. Technol. *109*, 25–31.

150. Nan, C.-W., Liu, G., Lin, Y., and Li, M. (2004). Interface effect on thermal conductivity of carbon nanotube composites. Appl. Phys. Lett. *85*, 3549–3551.

151. Goyal, V., and Balandin, A.A. (2012). Thermal properties of the hybrid graphene-metal nano-micro-composites: applications in thermal interface materials. Appl. Phys. Lett. *100*, 073113.

152. Wang, F., Zeng, X., Yao, Y., Sun, R., Xu, J., and Wong, C.P. (2016). Silver nanoparticle-deposited boron nitride nanosheets as fillers for polymeric composites with high thermal conductivity. Sci. Rep. *6*, 19394.

153. Suh, D., Moon, C.M., Kim, D., and Baik, S. (2016). Ultrahigh thermal conductivity of interface materials by silver-functionalized carbon nanotube phonon conduits. Adv. Mater. *28*, 7220–7227.

154. Chu, K., Li, W.-s., Jia, C.-c., and Tang, F.-l. (2012). Thermal conductivity of composites with hybrid carbon nanotubes and graphene nanoplatelets. Appl. Phys. Lett. *101*, 211903.

155. Kholmanov, I., Kim, J., Ou, E., Ruoff, R.S., and Shi, L. (2015). Continuous carbon nanotube–ultrathin graphite hybrid foams for increased thermal conductivity and suppressed subcooling in composite phase change materials. ACS Nano *9*, 11699–11707.

156. Pettes, M.T., Ji, H., Ruoff, R.S., and Shi, L. (2012). Thermal transport in three-dimensional foam architectures of few-layer graphene and ultrathin graphite. Nano Lett. *12*, 2959–2964.

157. Qiu, L., Liu, J.Z., Chang, S.L., Wu, Y., and Li, D. (2012). Biomimetic superelastic graphene-based cellular monoliths. Nat. Commun. *3*, 1241.

158. Yao, B., Chen, J., Huang, L., Zhou, Q., and Shi, G. (2016). Base-induced liquid crystals of graphene oxide for preparing elastic graphene foams with long-range ordered microstructures. Adv. Mater. *28*, 1623–1629.

159. Ji, H., Sellan, D.P., Pettes, M.T., Kong, X., Ji, J., Shi, L., and Ruoff, R.S. (2014). Enhanced thermal conductivity of phase change materials with ultrathin-graphite foams for thermal energy storage. Energy Environ. Sci. *7*, 1185–1192.

160. Xue, Y., Dai, P., Zhou, M., Wang, X., Pakdel, A., Zhang, C., Weng, Q., Takei, T., Fu, X., Popov, Z.I., et al. (2017). Multifunctional superelastic foam-like boron nitride nanotubular cellular-network architectures. ACS Nano *11*, 558–568.

161. Ashton, T.S., and Moore, A.L. (2017). Foam-like hierarchical hexagonal boron nitride as a non-traditional thermal conductivity enhancer for polymer-based composite materials. Int. J. Heat Mass Transf. *115*, 273–281.

162. Zeng, X., Yao, Y., Gong, Z., Wang, F., Sun, R., Xu, J., and Wong, C.P. (2015). Ice-templated assembly strategy to construct 3D boron nitride nanosheet networks in polymer composites for thermal conductivity improvement. Small *11*, 6205–6213.

163. Lian, G., Tuan, C.-C., Li, L., Jiao, S., Wang, Q., Moon, K.-S., Cui, D., and Wong, C.-P. (2016). Vertically aligned and interconnected graphene networks for high thermal conductivity of epoxy composites with ultralow loading. Chem. Mater. *28*, 6096–6104.

164. Ma, J., Zhou, X., Ding, S., and Liu, Z. (2017). Solvent evaporation induced self-assembly of graphene foam for thermally conductive polymers. RSC Adv. *7*, 15469–15474.

165. Hu, J., Huang, Y., Yao, Y., Pan, G., Sun, J., Zeng, X., Sun, R., Xu, J.B., Song, B., and Wong, C.P. (2017). Polymer composite with improved thermal conductivity by constructing a hierarchically ordered three-dimensional interconnected network of BN. ACS Appl. Mater. Inter. *9*, 13544–13553.

166. Hata, K., Futaba, D.N., Mizuno, K., Namai, T., Yumura, M., and Iijima, S. (2004). Water-assisted highly efficient synthesis of impurity-free single-walled carbon nanotubes. Science *306*, 1362–1364.

167. Wang, D., Song, P., Liu, C., Wu, W., and Fan, S. (2008). Highly oriented carbon nanotube papers made of aligned carbon nanotubes. Nanotechnology *19*, 075609.

168. Li, Q., Liu, C., and Fan, S. (2009). Thermal boundary resistances of carbon nanotubes in contact with metals and polymers. Nano Lett. *9*, 3805–3809.

169. Hu, M., Keblinski, P., Wang, J.-S., and Raravikar, N. (2008). Interfacial thermal conductance between silicon and a vertical carbon nanotube. J. Appl. Phys. *104*, 083503.

170. Varshney, V., Patnaik, S.S., Roy, A.K., Froudakis, G., and Farmer, B.L. (2010). Modeling of thermal transport in pillared-graphene architectures. ACS Nano *4*, 1153–1161.

171. Xu, L., Wei, N., Zheng, Y., Fan, Z., Wang, H.-Q., and Zheng, J.-C. (2012). Graphene-nanotube 3D networks: intriguing thermal and mechanical properties. J. Mater. Chem. *22*, 1435–1444.

172. Dimitrakakis, G.K., Tylianakis, E., and Froudakis, G.E. (2008). Pillared graphene: a new 3-D network nanostructure for enhanced hydrogen storage. Nano Lett. *8*, 3166–3170.

173. Zhu, Y., Li, L., Zhang, C., Casillas, G., Sun, Z., Yan, Z., Ruan, G., Peng, Z., Raji, A.R., Kittrell, C., et al. (2012). A seamless three-dimensional carbon nanotube graphene hybrid material. Nat. Commun. *3*, 1225.

174. Tang, C., Zhang, Q., Zhao, M.-Q., Tian, G.-L., and Wei, F. (2014). Resilient aligned carbon nanotube/graphene sandwiches for robust mechanical energy storage. Nano Energy *7*, 161–169.

175. Loeblein, M., Tsang, S.H., Pawlik, M., Phua, E.J., Yong, H., Zhang, X.W., Gan, C.L., and Teo, E.H. (2017). High-density 3D-boron nitride and 3D-graphene for high-performance nano-thermal interface material. ACS Nano *11*, 2033–2044.

176. Lv, P., Tan, X.-W., Yu, K.-H., Zheng, R.-L., Zheng, J.-J., and Wei, W. (2016). Super-elastic graphene/carbon nanotube aerogel: a novel thermal interface material with highly thermal transport properties. Carbon *99*, 222–228.

177. Yan, Z., Liu, G.X., Khan, J.M., and Balandin, A.A. (2012). Graphene quilts for thermal management of high-power GaN transistors. Nat. Commun. *3*, 827.

178. Shen, B., Zhai, W., and Zheng, W. (2014). Ultrathin flexible graphene film: an excellent thermal conducting material with efficient EMI shielding. Adv. Funct. Mater. *24*, 4542–4548.

179. Liang, Q., Yao, X., Wang, W., Liu, Y., and Wong, C.P. (2011). A three-dimensional vertically aligned functionalized multilayer graphene architecture: an approach for graphene-based thermal interfacial materials. ACS Nano *5*, 2392–2401.

180. Xin, G., Sun, H., Hu, T., Fard, H.R., Sun, X., Koratkar, N., Borca-Tasciuc, T., and Lian, J. (2014). Large-area freestanding graphene paper for superior thermal management. Adv. Mater. *26*, 4521–4526.

181. Teng, C., Xie, D., Wang, J., Yang, Z., Ren, G., and Zhu, Y. (2017). Ultrahigh conductive graphene paper based on ball-milling exfoliated graphene. Adv. Funct. Mater. *27*, https://doi.org/10.1002/adfm.201700240.

182. Zhao, J., Pei, S., Ren, W., Gao, L., and Cheng, H.M. (2010). Efficient preparation of large-area graphene oxide sheets for transparent conductive films. ACS Nano *4*, 5245–5252.

183. Zheng, Q., Ip, W.H., Lin, X., Yousefi, N., Yeung, K.K., Li, Z., and Kim, J.K. (2011). Transparent conductive films consisting of ultralarge graphene sheets produced by Langmuir-Blodgett assembly. ACS Nano *5*, 6039–6051.

184. Renteria, J.D., Ramirez, S., Malekpour, H., Alonso, B., Centeno, A., Zurutuza, A., Cocemasov, A.I., Nika, D.L., and Balandin, A.A. (2015). Strongly anisotropic thermal conductivity of free-standing reduced graphene oxide films annealed at high temperature. Adv. Funct. Mater. *25*, 4664–4672.

185. Song, L., Khoerunnisa, F., Gao, W., Dou, W., Hayashi, T., Kaneko, K., Endo, M., and Ajayan, P.M. (2013). Effect of high-temperature thermal treatment on the structure and adsorption properties of reduced graphene oxide. Carbon *52*, 608–612.

186. Kumar, P., Shahzad, F., Yu, S., Hong, S.M., Kim, Y.-H., and Koo, C.M. (2015). Large-area reduced graphene oxide thin film with excellent thermal conductivity and electromagnetic interference shielding effectiveness. Carbon *94*, 494–500.

187. Hishiyama, Y., Nakamura, M., Nagata, Y., and Inagaki, M. (1994). Graphitization behavior of carbon film prepared from high modulus polyimide film: synthesis of high-quality graphite film. Carbon *32*, 645–650.

188. Kong, Q.Q., Liu, Z., Gao, J.G., Chen, C.M., Zhang, Q., Zhou, G., Tao, Z.C., Zhang, X.H., Wang, M.Z., and Li, F. (2014). Hierarchical graphene–carbon fiber composite paper as a flexible lateral heat spreader. Adv. Funct. Mater. *24*, 4222–4228.

189. Wu, H., and Drzal, L.T. (2012). Graphene nanoplatelet paper as a light-weight composite with excellent electrical and thermal conductivity and good gas barrier properties. Carbon *50*, 1135–1145.

190. Qin, M., Feng, Y., Ji, T., and Feng, W. (2016). Enhancement of cross-plane thermal conductivity and mechanical strength via vertical aligned carbon nanotube@ graphite architecture. Carbon *104*, 157–168.

191. Zhang, J., Shi, G., Jiang, C., Ju, S., and Jiang, D. (2015). 3D bridged carbon nanoring/graphene hybrid paper as a high-performance lateral heat spreader. Small *11*, 6197–6204.

192. Xu, Z., Liu, Z., Sun, H., and Gao, C. (2013). Highly electrically conductive Ag-doped graphene fibers as stretchable conductors. Adv. Mater. *25*, 3249–3253.

193. Meng, Y., Zhao, Y., Hu, C., Cheng, H., Hu, Y., Zhang, Z., Shi, G., and Qu, L. (2013). All-graphene core-sheath microfibers for all-solid-state, stretchable fibriform supercapacitors and wearable electronic textiles. Adv. Mater. *25*, 2326–2331.

194. Xu, Z., Liu, Y., Zhao, X., Peng, L., Sun, H., Xu, Y., Ren, X., Jin, C., Xu, P., and Wang, M. (2016). Ultrastiff and strong graphene fibers via full-scale synergetic defect engineering. Adv. Mater. *28*, 6449–6456.

195. Xin, G., Yao, T., Sun, H., Scott, S.M., Shao, D., Wang, G., and Lian, J. (2015). Highly thermally conductive and mechanically strong graphene fibers. Science *349*, 1083–1087.

196. Qin, X., Lu, Y., Xiao, H., Wen, Y., and Yu, T. (2012). A comparison of the effect of graphitization on microstructures and properties of polyacrylonitrile and mesophase pitch-based carbon fibers. Carbon *50*, 4459–4469.

197. Ackerman, C.C., Bertman, B., Fairbank, H.A., and Guyer, R. (1966). Second sound in solid helium. Phys. Rev. Lett. *16*, 789.

198. Ward, J., and Wilks, J., III (1952). Second sound and the thermo-mechanical effect at very low temperatures. Lond. Edinb. Dublin Philos. Mag. J. Sci. *43*, 48–50.

199. Dresselhaus, M.S., Chen, G., Tang, M.Y., Yang, R., Lee, H., Wang, D., Ren, Z., Fleurial, J.P., and Gogna, P. (2007). New directions for low-dimensional thermoelectric materials. Adv. Mater. *19*, 1043–1053.

200. Kim, T.Y., Park, C.H., and Marzari, N. (2016). The electronic thermal conductivity of graphene. Nano Lett. *16*, 2439–2443.

201. Zhang, J., Hong, Y., and Yue, Y. (2015). Thermal transport across graphene and single layer hexagonal boron nitride. J. Appl. Phys. *117*, 134307.

202. Zheng, K., Sun, F., Zhu, J., Ma, Y., Li, X., Tang, D., Wang, F., and Wang, X. (2016). Enhancing the thermal conductance of polymer and sapphire interface via self-assembled monolayer. ACS Nano *10*, 7792–7798.

203. Marconnet, A.M., Panzer, M.A., and Goodson, K.E. (2013). Thermal conduction phenomena in carbon nanotubes and related nanostructured materials. Rev. Mod. Phys. *85*, 1295.

204. Panzer, M., Zhang, G., Mann, D., Hu, X., Pop, E., Dai, H., and Goodson, K. (2008). Thermal properties of metal-coated vertically aligned single-wall nanotube arrays. J. Heat Transfer *130*, 052401.

205. Li, Z., Wu, P., Wang, C., Fan, X., Zhang, W., Zhai, X., Zeng, C., Li, Z., Yang, J., and Hou, J. (2011). Low-temperature growth of graphene by chemical vapor deposition using solid and liquid carbon sources. ACS Nano *5*, 3385–3390.